Complete Genome Sequencing of *Acinetobacter baumannii* AC1633 and *Acinetobacter nosocomialis* AC1530 Unveils a Large Multidrug-Resistant Plasmid Encoding the NDM-1 and OXA-58 Carbapenemases

Ahmed Ghazi Alattraqchi,[a] Farahiyah Mohd Rani,[a] Nor Iza A. Rahman,[a] Salwani Ismail,[a] David W. Cleary,[b,c] Stuart C. Clarke,[b,c,d,e,f] Chew Chieng Yeo[a]

[a]Faculty of Medicine, Universiti Sultan Zainal Abidin, Kuala Terengganu, Terengganu, Malaysia
[b]Faculty of Medicine and Institute for Life Sciences, University of Southampton, Southampton, United Kingdom
[c]NIHR Southampton Biomedical Research Centre, University Hospital Southampton NHS Trust, Southampton, United Kingdom
[d]Global Health Research Institute, University of Southampton, Southampton, United Kingdom
[e]School of Postgraduate Studies, International Medical University, Kuala Lumpur, Malaysia
[f]Centre for Translational Research, IMU Institute for Research, Development and Innovation (IRDI), Kuala Lumpur, Malaysia

Ahmed Ghazi Alattraqchi and Farahiyah Mohd Rani contributed equally to this work. Author order was determined alphabetically.

ABSTRACT Carbapenem-resistant *Acinetobacter* spp. are considered priority drug-resistant human-pathogenic bacteria. The genomes of two carbapenem-resistant *Acinetobacter* spp. clinical isolates obtained from the same tertiary hospital in Terengganu, Malaysia, namely, *A. baumannii* AC1633 and *A. nosocomialis* AC1530, were sequenced. Both isolates were found to harbor the carbapenemase genes bla_{NDM-1} and bla_{OXA-58} in a large (ca. 170 kb) plasmid designated pAC1633-1 and pAC1530, respectively, that also encodes genes that confer resistance to aminoglycosides, sulfonamides, and macrolides. The two plasmids were almost identical except for the insertion of IS*Aba11* and an IS*4* family element in pAC1633-1, and IS*Aba11* along with *relBE* toxin-antitoxin genes flanked by inversely orientated p*dif* (XerC/XerD) recombination sites in pAC1530. The bla_{NDM-1} gene was encoded in a Tn*125* composite transposon structure flanked by IS*Aba125*, whereas bla_{OXA-58} was flanked by IS*Aba11* and IS*Aba3* downstream and a partial IS*Aba3* element upstream within a p*dif* module. The presence of conjugative genes in plasmids pAC1633-1/pAC1530 and their discovery in two distinct species of *Acinetobacter* from the same hospital are suggestive of conjugative transfer, but mating experiments failed to demonstrate transmissibility under standard laboratory conditions. Comparative sequence analysis strongly inferred that pAC1633-1/pAC1530 was derived from two separate plasmids in an IS*1006*-mediated recombination or transposition event. *A. baumannii* AC1633 also harbored three other plasmids designated pAC1633-2, pAC1633-3, and pAC1633-4. Both pAC1633-3 and pAC1633-4 are cryptic plasmids, whereas pAC1633-2 is a 12,651-bp plasmid of the GR8/GR23 Rep3 superfamily group that encodes the *tetA*(39) tetracycline resistance determinant in a p*dif* module.

IMPORTANCE Bacteria of the genus *Acinetobacter* are important hospital-acquired pathogens, with carbapenem-resistant *A. baumannii* listed by the World Health Organization as the one of the top priority pathogens. Whole-genome sequencing of carbapenem-resistant *A. baumannii* AC1633 and *A. nosocomialis* AC1530, which were isolated from the main tertiary hospital in Terengganu, Malaysia, led to the discovery of a large, ca. 170-kb plasmid that harbored genes encoding the New Delhi metallo-β-lactamase-1 (NDM-1) and OXA-58 carbapenemases alongside genes that conferred

resistance to aminoglycosides, macrolides, and sulfonamides. The plasmid was a patchwork of multiple mobile genetic elements and comparative sequence analysis indicated that it may have been derived from two separate plasmids through an IS*1006*-mediated recombination or transposition event. The presence of such a potentially transmissible plasmid encoding resistance to multiple antimicrobials warrants vigilance, as its spread to susceptible strains would lead to increasing incidences of antimicrobial resistance.

KEYWORDS NDM-1, OXA-58, carbapenem resistance, Tn125, p*dif* modules, *Acinetobacter baumannii*, *Acinetobacter nosocomialis*, plasmids

Infections caused by the Gram-negative pathogen *Acinetobacter baumannii* have become increasingly problematic, particularly among immunocompromised patients and patients in intensive care units, due to its ability to acquire and develop resistance to multiple antimicrobials and thereby severely limit treatment options (1, 2). The genomes of *Acinetobacter* strains are flexible and adaptable, prone to accumulating antibiotic resistance determinants through horizontal gene transfer involving mobile genetic elements (3, 4). Resistance to carbapenems, which are among the antimicrobials of last resort for the treatment of multidrug-resistant (MDR) *Acinetobacter* infections, is increasing, with resistance rates exceeding 90% in certain regions of the world (5). Of pressing concern, pandrug-resistant (PDR) isolates of *A. baumannii*, which are resistant to all classes of antimicrobials, have been reported from clinical as well as environmental samples (6–8). In the CDC's 2019 Antibiotic Resistance Threats Report, carbapenem-resistant *A. baumannii* has been listed as an "urgent" threat (9). Likewise, the World Health Organization (WHO) has categorized carbapenem-resistant *A. baumannii* as a critical priority pathogen toward which new antimicrobials are urgently needed (10).

A. nosocomialis is closely related to *A. baumannii* and, along with *A. pittii*, *A. seifertii*, *A. dijkshoorniae*, and *A. calcoaceticus*, they are often grouped together as the *A. baumannii-A. calcoaceticus* (Abc) complex due to difficulties in identifying these bacteria by traditional biochemical methods (11, 12). In our recent study of *Acinetobacter* isolates obtained from the main tertiary hospital in the state of Terengganu, Malaysia in 2015, the majority (83.7%) were *A. baumannii* followed by *A. nosocomialis* (10.4%), with multidrug resistance much more prevalent in *A. baumannii* (13). Nevertheless, *A. nosocomialis* and other members of the Abc complex are clinically relevant, with carbapenem-resistant and MDR isolates being reported (14).

Multiple mechanisms of drug resistance are usually at play in *Acinetobacter* isolates and these include enzymatic inactivation of the antibiotic, modifications in the target sites, reduced accumulation of antibiotics through expression of efflux systems or mutations in outer membrane channels, and the formation of biofilms (15, 16). Carbapenem resistance in *Acinetobacter* is frequently attributed to the acquisition and production of OXA β-lactamases, which are categorized as Ambler class D enzymes with a serine residue within the active site that catalyzes the hydrolysis of the β-lactam substrate (17). Common acquired OXA subtypes found in *Acinetobacter* include OXA-23, OXA-24/40, OXA-58, OXA-143, and OXA-235, with the genes encoding them usually associated with or located in mobile genetic elements (16, 17). In some instances, an upstream and adjacent insertion sequence (IS) element provides a strong outward-directing promoter for their expression (17). *A. baumannii* also harbors an intrinsic $bla_{OXA-51}/bla_{OXA-51-like}$ gene in its chromosome and, although the OXA-51/OXA-51-like enzyme has been shown to hydrolyze imipenem and meropenem, its affinity for these carbapenems is quite low and would not normally confer carbapenem resistance (17). However, the insertion of IS elements with outward-directing promoters, such as IS*Aba1*, upstream of the $bla_{OXA-51}/bla_{OXA-51-like}$ gene has been shown to increase expression of the enzyme, leading to carbapenem resistance (18). Nevertheless, recent reports have indicated that in the absence of an acquired carbapenemase gene, the presence of IS*Aba1* or similar elements upstream and adjacent to the intrinsic $bla_{OXA-51}/$

$bla_{OXA-51-like}$ gene does not always guarantee carbapenem resistance in these isolates (13, 19).

The metallo-β-lactamases (MBLs) or Ambler class B enzymes, such as the New Delhi metallo-β-lactamase (NDM) group, represents another class of acquired carbapenemases that have been found in *Acinetobacter* spp., being first reported in *A. baumannii* from India (20) and China (21). MBLs, including NDMs, are dependent on zinc ions at the active site of the enzyme (16). The bla_{NDM-1} gene has since been found in many other *Acinetobacter* spp., is usually carried in the composite transposon Tn125 or its derivatives, and is either plasmid- or chromosome-encoded (22). NDM-1 confers resistance to all β-lactams except monobactams, such as aztreonam, and is not inhibited by β-lactamase inhibitors such as clavulanic acid, sulbactam, tazobactam, and avibactam (16, 23, 24). Most isolates that harbor the bla_{NDM-1} gene are likely MDR or extensive-drug resistant (XDR) due to the association of bla_{NDM-1} with other resistance genes (16, 22).

Here, we report the whole-genome sequences of two NDM-1-producing, carbapenem-resistant *Acinetobacter* clinical isolates, *A. baumannii* AC1633 and *A. nosocomialis* AC1530, obtained from the main tertiary hospital in the state of Terengganu in Peninsular Malaysia. We show that in these two isolates, the bla_{NDM-1} gene is colocated with bla_{OXA-58} on a large ca. 170-kb plasmid along with various other antimicrobial-resistance genes, and that the carriage of this plasmid in these two isolates likely led to their MDR status. We also show sequence evidence that this plasmid was likely derived from two plasmids that separately encoded bla_{NDM-1} and bla_{OXA-58} in a Malaysian *A. pittii* isolate and that they combined via an IS1006-mediated recombination event.

RESULTS AND DISCUSSION

Background of the *A. baumannii* AC1633 and *A. nosocomialis* AC1530 clinical isolates. *A. baumannii* AC1633 and *A. nosocomialis* AC1530 are part of our collection of *Acinetobacter* spp. clinical isolates that were obtained since 2011 from Hospital Sultanah Nur Zahirah (HSNZ), the main public tertiary hospital in the state of Terengganu, Malaysia (13, 25). Whole-genome sequencing was performed on a random selection of 50 isolates obtained from 2011 to 2016 (manuscript in preparation) and preliminary analyses of the genome sequences indicated two isolates that harbored the bla_{NDM-1} gene, i.e., AC1633 and AC1530.

A. baumannii AC1633 was isolated from the blood of a 60-year-old female patient in the neurology intensive care unit in April 2016. The patient had hospital-acquired pneumonia with respiratory failure and eventually succumbed to septicemia 41 days after hospital admission. *A. nosocomialis* AC1530 was isolated from the blood of a 14-year-old male patient in the surgical ward in April 2015. The patient was admitted for polytrauma due to a motor vehicle accident and developed hospital-acquired pneumonia complicated with right parapneumonic effusion, but recovered and was discharged after 60 days. *A. baumannii* AC1633 was resistant to the carbapenems (with imipenem, meropenem, and doripenem MIC values of >32 µg/ml each), cephalosporins (cefotaxime, ceftriaxone, ceftazidime, and cefepime), β-lactam/β-lactamase inhibitor combinations (piperacillin-tazobactam and ampicillin-sulbactam), trimethoprim-sulfamethoxazole, ciprofloxacin, and tetracycline. AC1633 also showed resistance to gentamicin but was susceptible to the other aminoglycosides tested (namely, amikacin and tobramycin), as well as to levofloxacin, doxycycline, and the polymyxins (polymyxin B and colistin). *A. nosocomialis* AC1530 was resistant to the carbapenems (with MIC values for imipenem, meropenem, and doripenem of >32 µg/ml each), cephalosporins (cefotaxime, ceftriaxone, ceftazidime, and cefepime), trimethoprim-sulfamethoxazole, and gentamicin, but was susceptible to all other antibiotics tested. Thus, both AC1633 and AC1530 are categorized as MDR following the criteria proposed by the joint commission of the U.S. Centers for Disease Control and Prevention (CDC) and the European Centre for Disease Prevention and Control (ECDC) (26).

Whole-genome sequencing and comparative analyses of AC1633 and AC1530. Analysis of the Illumina-sequenced genomes of *A. baumannii* A1633 and *A. nosocomialis* AC1530 indicated the presence of the bla_{NDM-1} and bla_{OXA-58} carbapenemase genes.

TABLE 1 Genome features of *A. baumannii* AC1633 and *A. nosocomialis* AC1530

Feature	A. baumannii AC1633					A. nosocomialis AC1530	
	Chromosome	pAC1633-1	pAC1633-2	pAC1633-3	pAC1633-4	Chromosome	pAC1530
Size (bp)	4,364,474	174,292	12,651	9,950	5,210	3,980,182	173,972
% GC content	39	38	36	36	37	38	38
Total no. of genes	2,112	29	4		1	1,918	29
No. of rRNA operons	18					18	
No. of tRNAs	72					74	
Total no. of coding sequences (CDS)	4,096	176	18	13	8	3,750	180

Production of the NDM-1 metallo-β-lactamase (MBL) in both isolates was validated by testing with the Etest MBL kit (bioMérieux). Further analyses of the assembled genome data of AC1530 and AC1633 revealed the possibility that the bla_{NDM-1} and bla_{OXA-58} genes could be harbored in either one or two large plasmids in both isolates; however, this was difficult to ascertain as there were more than 20 assembled contigs from each isolate's genome data that could potentially belong to these plasmids. Thus, the genomic DNA of these two isolates was subjected to PacBio sequencing and hybrid assembly was then performed on the PacBio and Illumina reads. The resulting assembled genome features of these two isolates are listed in Table 1.

The genome of *A. baumannii* AC1633 is nearly 4.4 Mb in size and is comprised of a single chromosome of 4.36 Mb (accession no. CP059300) and four plasmids designated pAC1633-1 (174 kb; CP059301), pAC1633-2 (12.6 kb; CP059303), pAC1633-3 (9.9 kb; CP059304), and pAC1633-4 (5.2 kb; CP059302). *A. baumannii* AC1633 is typed as ST2089 under the Oxford multilocus sequence type (MLST) scheme and ST126 under the Pasteur MLST scheme. AC1633 does not belong to any of the major *A. baumannii* global clonal lineages, and phylogenetic analysis of the whole-genome sequence in comparison with the sequences of selected *A. baumannii* isolates (Fig. 1A, Table S1 in the supplemental material) showed it is most closely related to *A. baumannii* CIP70.10 (ATCC 15151), which was isolated in France in 1970 and is an important reference strain due to its susceptibility to most antimicrobials (27). CIP70.10 also belonged to the same STs as AC1633. Phylogenetic analyses also indicated that AC1633 is not closely related to any of the few Malaysian *A. baumannii* genomes that are currently available in the database, most of which belonged to the Global Clonal 2 (GC2) lineage (28, 29). *A. baumannii* isolates AC12, AC29, and AC30, which were isolated from the same hospital as AC1530 and AC1633 but in the year 2011, were of the sequence type ST195 (Oxford)/ST2 (Pasteur) (30, 31). A recent report of 13 *A. baumannii* genomes from Malaysia indicated three isolates that harbored bla_{NDM-1} (29); however, we were unable to compare these isolates with ours as the sequence files that were associated with the GenBank accession numbers provided in the manuscript have yet to be publicly released at the time of writing (December 24, 2020). Using the KAPTIVE database that enables the typing of *A. baumannii* strains by variation in their composition and structure of capsular polysaccharide (CPS) biosynthetic genes (32), AC1633 was typed as OCL6 for the outer core biosynthesis locus and KL14 for the K locus, which contain genes responsible for the biosynthesis and export of CPS, and both loci were typed with 100% match confidence level.

A. nosocomialis AC1530 has a single chromosome of 3.98 Mb (CP045560.1) and a plasmid of 173.9 kb designated pAC1530 (CP045561.1). AC1530 was assigned by the curators of the PubMLST database (33) to the Pasteur ST1539 (with alleles *cpn60*-47, *fusA*-26, *gltA*-50, *pyrG*-14, *recA*-26, *rplB*-16, and *rpoB*-49) and Oxford ST2195 (with alleles *cpn60*-73, *gdhB*-86, *gltA*-76, *gpi*-4, *gyrB*-65, *recA*-21, and *rpoD*-90). Phylogenetic analyses showed that the closest relative of AC1530 is *A. nosocomialis* T228 (accession no. JRUA01000001.1), a clinical isolate obtained from Bangkok, Thailand in 2010 (Fig. 1B, Table S1). However, *A. nosocomialis* T228 was typed as Pasteur ST279 and Oxford ST1897, whereas AC1530 shared only a single allele in the Oxford scheme (*gyrB*-65) and two alleles in the Pasteur scheme (*fusA*-26, *rplB*-16) with T228.
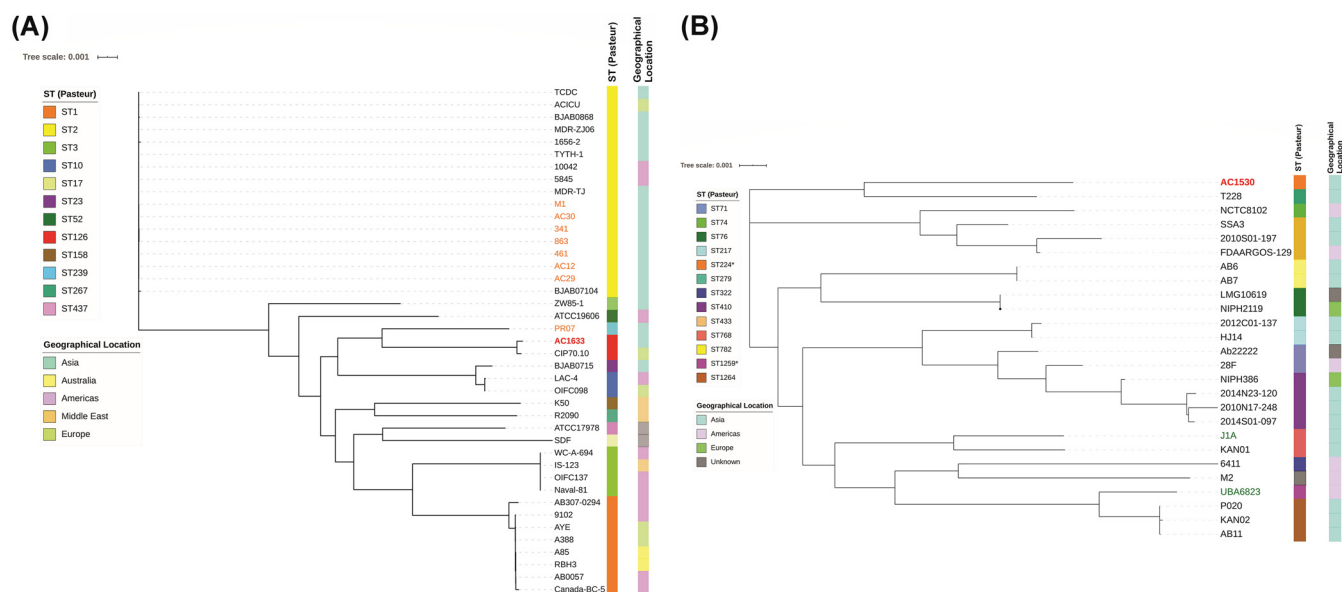
FIG 1 Core genome phylogenetic trees of *A. baumannii* AC1633 (A) and *A. nosocomialis* AC1530 (B) in comparison with other related isolates. The *A. baumannii* core genome comprises 1,167 genes from a total of 20,102 genes, whereas the *A. nosocomialis* core genome consisted of 1,147 genes from a total of 18,024 genes. The sequence types (STs) of the isolates as determined using the Pasteur scheme are presented by the colored bar on the immediate right of the respective trees. For *A. baumannii* in (A), ST1 corresponds to the global clone 1 (GC1) lineage, ST2 to GC2 and ST3 to GC3. The geographical location of the respective isolates is also presented as a colored bar on the furthest right of each tree. In (A), *A. baumannii* isolates from Malaysia are indicated in orange fonts (except AC1633, which is indicated in bold red font) and in (B), *A. nosocomialis* environmental isolates are indicated in blue-green fonts. All other *A. nosocomialis* isolates were obtained from clinical samples. Details of the *A. baumannii* and *A. nosocomialis* isolates that were used in the phylogenetic analyses are in Table S1 in the supplemental material.

Antimicrobial resistance genes in the genomes of AC1633 and AC1530. Interestingly, the bulk of the acquired antimicrobial resistance genes for *A. baumannii* AC1633 and *A. nosocomialis* AC1530 came from the large ca. 170-kb plasmid, pAC1633-1 and pAC1530, respectively (Table 2). *A. baumannii* AC1633 harbored two β-lactam resistance genes in its chromosome, i.e., the intrinsic $bla_{OXA-51-like}$ gene categorized as $bla_{OXA-116}$ and the *Acinetobacter*-derived AmpC cephalosporinase (ADC) gene bla_{ADC-25} (accession no. EF016355.1) (34). In some cases, carbapenem resistance and increased cephalosporin resistance have been linked with upregulation of the respective $bla_{OXA-51}/bla_{OXA-51-like}$ or bla_{ADC} genes through insertion of IS*Aba1* or related IS elements that harbor outward-directing promoters (18, 35, 36); however, no such IS elements could be found upstream of the $bla_{OXA-116}$ and bla_{ADC-25} genes in *A. baumannii* AC1633. Tetracycline resistance in AC1633 is likely mediated by the *tetA*(39) gene that was carried on the smaller 12.6-kb plasmid, pAC1633-2 (Table 2), and that encodes the tetracycline-specific TetA(39) efflux pump of the major facilitator superfamily (MFS). Notably, pAC1633-1 also harbors the *adeABC* operon that encodes the multidrug resistance-nodulation-cell division (RND) family efflux system along with its two-component regulatory system, *adeRS*, which is located upstream and transcribed divergently from *adeABC*. This efflux system is usually chromosome encoded in *Acinetobacter* and the multidrug resistance phenotype has been shown to correlate with overexpression of *adeABC* (37, 38). Interestingly, the *A. baumannii* AC1633 chromosome harbors another copy of *adeRS* and *adeAB* (nucleotides [nt] 1011642 to 1016860), but *adeC* was absent. There were no obvious signs of mobile elements or genomic islands in the vicinity of the chromosomal *adeRS-adeAB* genes that could explain the deletion of *adeC*. The chromosome of AC1633 also harbors genes encoding the other *Acinetobacter* RND family efflux pumps *adeFGH* and *adeIJK*, along with their respective regulatory genes *adeL* and *adeN* (37, 39), three genes encoding MFS efflux pumps, i.e., *abaF*, *abaQ*, and *amvA*, and, finally, *abeS*, which encodes a small-multidrug resistance (SMR) family efflux pump (Table 3).

As for *A. nosocomialis* AC1530, very few antimicrobial resistance genes are found in its chromosome, and the only resistance gene encoding an antibiotic-inactivating

TABLE 2 Antimicrobial resistance phenotype and carriage of antimicrobial resistance genes and chromosomal gene mutations in *A. baumannii* AC1633 and *A. nosocomialis* AC1530

Strain	Antimicrobial resistance phenotype by class/carriage of resistance genes or chromosomal mutations[b]						
	Carbapenems	Cephalosporins	Aminoglycosides	Tetracyclines	Fluoroquinolones	Sulfonamides	Macrolides
A. baumannii AC1633							
Chromosome	IMI[R] MEM[R] DOR[R] bla_{OXA116} ($bla_{OXA-51-like}$)	CTX[R] FOX[R] TAZ[R] FEP[R] bla_{ADC-25}	GEN[R] AMI[S] TOB[S]	TET[R] DOX[S]	CIP[R] LEV[S] $gyrA$ S81L[a], $parC$ V104I D105E[a]	SXT[R]	ND
pAC1633-1	bla_{NDM-1}, bla_{OXA-58}						
pAC1633-2			$aac(3)$-IId, $aph(3'')$-Ib, $aph(6)$-Id	$tetA(39)$		$sul2$	$msrE$, $mphE$
pAC1633-3							
pAC1633-4							
A. nosocomialis AC1530							
Chromosome	IMI[R] MEM[R] DOR[R]	CTX[R] FOX[R] TAZ[R] FEP[R] bla_{ADC-68}	GEN[R] AMI[S] TOB[S]	TET[S] DOX[S]	CIP[S] LEV[S] $parC$ V104I D105E[a]	SXT[R]	ND
pAC1530	bla_{NDM-1}, bla_{OXA-58}		$aac(3)$-IId, $aph(3'')$-Ib, $aph(6)$-Id			$sul2$	$msrE$, $mphE$

[a]Mutations in the chromosomally encoded *gyrA* and *parC* genes.

[b]IMI, imipenem; MEM, meropenem; DOR, doripenem; CTX, cefotaxime; FOX, cefoxitin; CTX, ceftriaxone; TAZ, ceftazidime; FEP, cefepime; GEN, gentamicin; AMI, amikacin; TOB, tobramycin; TET, tetracycline; DOX, doxycycline; CIP, ciprofloxacin; LEV, levofloxacin; SXT, trimethoprim-sulfamethoxazole; ND, not determined; R, resistance; I, intermediate resistance; S, susceptible.

TABLE 3 Carriage of efflux-mediated antimicrobial resistance genes in *A. baumannii* AC1633 and *A. nosocomialis* AC1530

	Efflux pump family		
Strain	Resistance-nodulation division (RND) family[a]	Major facilitator superfamily (MFS)	Small multidrug resistance (SMR) family
A. baumannii AC1633			
Chromosome	*adeI, adeJ, adeK, adeN, adeF, adeG, adeH, adeL, adeR, adeS, adeA, adeB*	*abaF, abaQ, amvA*	*abeS*
pAC1633-1	*adeR, adeS, adeA, adeB, adeC*		
pAC1633-2 pAC1633-3 pAC1633-4		*tetA(39)*	
A. nosocomialis AC1530			
Chromosome	*adeF, adeG, adeH, adeL, adeR, adeS, adeA, adeB, adeC*	*amvA, abaQ*	*abeS*
pAC1530	*adeR, adeS, adeA, adeB, adeC*		

[a]Genes in the same colored font indicate that they are part of an operon.

enzyme is a *bla*$_{ADC}$-encoding cephalosporinase that shared 94% amino acid sequence identity with ADC-68 (accession no. AGL39360.1) (40). However, as in the *A. baumannii* AC1633 genome, no IS elements with outward-directing promoters could be detected upstream of this gene. In contrast to AC1633, the chromosome of *A. nosocomialis* AC1530 harbored a full copy of the *adeRS-adeABC* efflux system besides the copy that resides on pAC1530. Other efflux pumps found encoded in the AC1530 chromosome are *adeFGH* and its regulatory gene *adeL*, the MFS superfamily pumps *amvA* and *abaQ*, and the SMR family *abeS* (Table 3). The same suite of resistance genes in pAC1633-1 was found in pAC1530 (Table 2) and, therefore, likely contributes to its resistance phenotype.

Characteristics of pAC1633-1 and pAC1530 and their carriage of antimicrobial resistance genes. Plasmids pAC1653-1 from *A. baumannii* AC1633 and pAC1530 from *A. nosocomialis* AC1530 were nearly identical except at five regions as follows (Fig. 2): (i) insertion of IS*Aba11* into an open reading frame (ORF) encoding an 85-aa (amino acid) hypothetical protein (locus tag: GD578_19675; accession no. QGA46103.1) which contains a ribosomal protein L7/L12 C-terminal domain (pfam00542) in pAC1530 at nt 40824 (nt 40825 to 41927 of pAC1633-1); this ORF is upstream of the *traMNO* genes and lies within a cluster of genes that are proposed to be part of the conjugative transfer region for the plasmid; (ii) an IS*4* family transposase at nt 58863 to 60133 in pAC1633-1 with no matches to existing IS elements in the ISFinder database (41) and no inverted repeats flanking the putative transposase gene; this is likely a remnant of an IS element that had inserted within IS*Aba31*, leading to only a partial IS*Aba31* downstream of this IS*4*-family remnant element (a full-length IS*Aba31* is found in the corresponding site in pAC1530 with a characteristic 2-bp "TA" direct repeat flanking the IS element); (iii) a 255-bp insertion within a hypothetical ORF at nt 89589 of pAC1530 in pAC1633-1 (nt 91978 to 92233); no characteristic signature sequences of mobile elements could be detected within this short fragment; (iv) insertion of IS*Aba11* into an ORF encoding a putative toxin of the Zeta toxin family in pAC1530; this insertion, at nt 101270 of pAC1633-1, led to a 5-bp direct repeat (TATAG) in pAC1530 (nt 98631 to 99731); and (v) addition of an *relBE* toxin-antitoxin (TA) system along with a
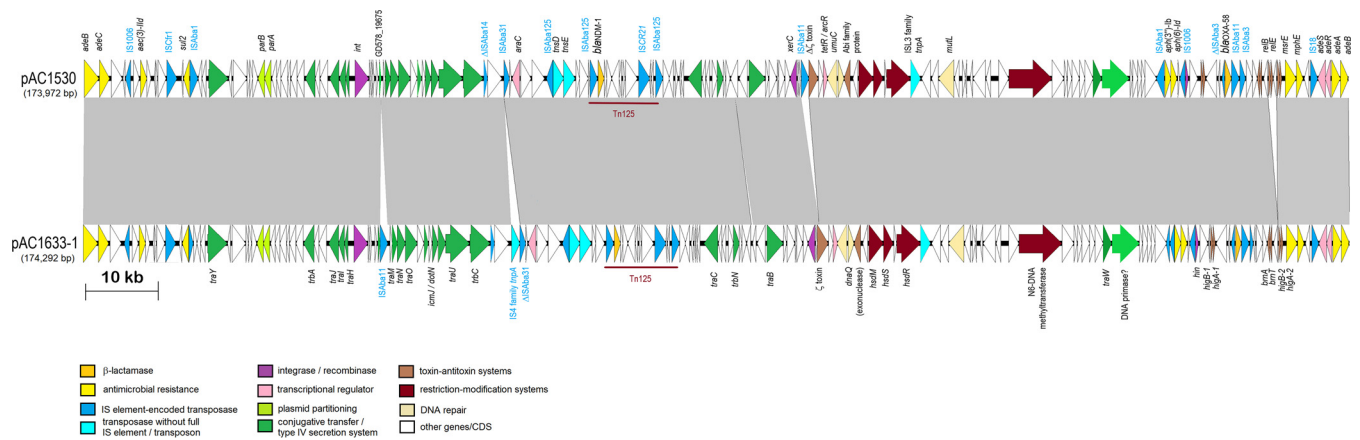
FIG 2 Comparative linear map of plasmids pAC1633-1 and pAC1530. Arrows indicate the extents and directions of genes and ORFs. The bla_{NDM-1} and bla_{OXA-58} genes are colored in gold, other antimicrobial resistance genes are in yellow. Putative transcriptional activators are in pink, including the genes encoding the two-component regulatory proteins *adeR* and *adeS* that control transcription of the *adeABC* efflux pump. Transposases encoded by full-copy IS elements are shown in dark blue, whereas transposases without their corresponding IS elements or transposons in full are depicted in light blue. Genes with homology to conjugative transfer or type IV secretion system genes are in dark green. GD578_19675 refers to the ORF in the conjugative region of pAC1530 that was the site of insertion for IS*Aba11* in pAC1633-1. Color codes for the other genes are as indicated. Tn*125* that harbors the bla_{NDM-1} gene is labeled. The extent of regions with >99% nucleotide sequence identities are indicated in the gray-shaded area.

downstream ORF encoding a protein of the SMI1/KNR4 family in pAC1530 at nt 164446 of pAC1633-1; this 1,192-bp fragment is flanked by p*dif* (XerD/XerC) recombination sites, more of which will be discussed in a later section. pAC1633-1 and pAC1530 belong to a group of diverse *Acinetobacter* plasmids that do not have an identifiable replication initiator or replicase (Rep) protein (42, 43).

Both pAC1633-1 and pAC1530 represent a repository of several antimicrobial resistance genes, including the bla_{NDM-1} and bla_{OXA-58} carbapenemase genes (Table 2). Three aminoglycoside resistance genes were found in both plasmids and all three encoded aminoglycoside-modifying enzymes. The *aac(3)-IId* group is a subclass of the AAC(3) enzymes that catalyze acetylation of the NH_2 group at the 3-position of the aminoglycoside 2-deoxystreptamine nucleus and usually confers resistance to gentamicin, sisomicin, and fortimicin (44). Both *A. baumannii* AC1633 and *A. nosocomialis* AC1530 were gentamicin resistant, but their susceptibilities against sisomicin and fortimicin were not tested. The other two aminoglycoside resistance genes found in pAC1633-1 and pAC1530 encode the aminoglycoside *O*-phophotransferases (APHs), *aph(6)-Id* and *aph(3″)-Ib*, and both genes confer resistance to streptomycin (44) (which was, however, not phenotypically tested in these *Acinetobacter* strains). Both genes were adjacent to each other and are flanked by IS elements, with IS*Aba1* upstream of *aph(3″)-Ib* and IS*1006* downstream of *aph(6)-Id* (Fig. 2).

The *sul2* gene that encodes dihydropteroate synthase, which confers sulfonamide resistance, is sandwiched between IS*Aba1* upstream and IS*Cfr1* downstream in both pAC1633-1 and pAC1530 (Fig. 2). In the chromosome of *A. baumannii* ATCC 19606, *sul2* is associated with the IS*CR2* element and is part of a large (36,157 bp) genomic island designated GI*sul2* (45). The association of *sul2* with the IS*CR2* element was previously reported in the plasmid RSF1010 (46). However, in the GC1 *A. baumannii* RUH875, IS*Aba1* was detected upstream of *sul2* and provided a promoter for its expression (47). This was observed in pAC1633-1 and pAC1530, except in these two plasmids, the IS*CR2* element was truncated due to the insertion of the 1,617-bp IS*Cfr1*.

The three aminoglycoside resistance genes, *aac(3)-IId*, *aph(6)-Id* and *aph(3′′)-Ib*, along with the *sul2* gene, were found to be in a 42,125-bp fragment in pAC1530 that was flanked by IS*Aba1* with characteristic 9-bp direct repeats of the target sequence in a typical composite transposon-like structure. This 42-kb fragment also included the bla_{OXA-58}, *msrE*, *mphE*, and *adeRS-adeABC* resistance genes that were nested in a 29,670-bp fragment flanked by IS*1006* (Fig. 3) and which is postulated to be derived from a smaller, separate plasmid via IS*1006*-mediated recombination/transposition. Comparative
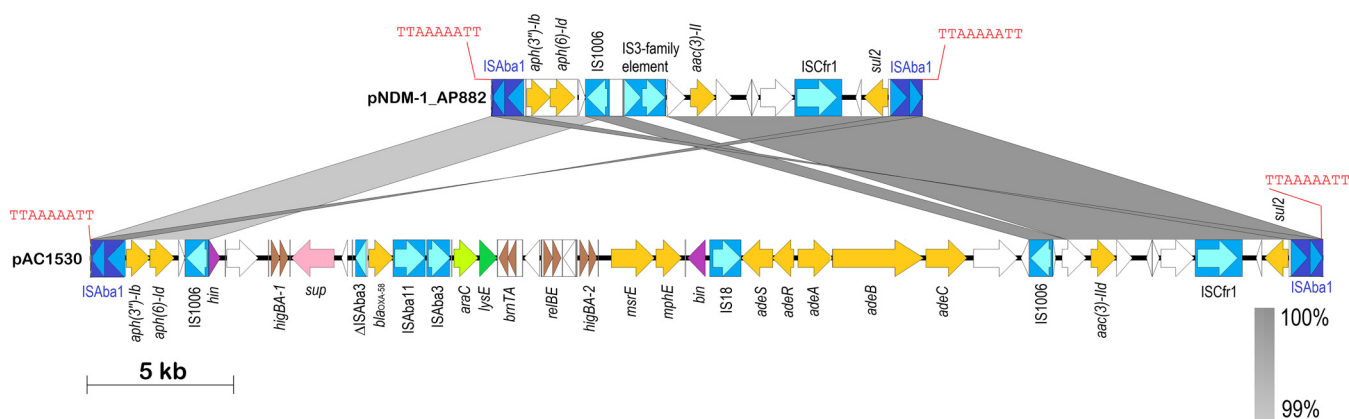
FIG 3 Linear map of the ISAba1-flanked composite transposon Tn6948 in the *A. pittii* AP882-derived plasmid pNDM-1_AP882 in comparison with the transposon in pAC1530. Arrows indicate extents and directions of genes and ORFs. Insertion sequence (IS) elements are depicted as blue-colored boxes with lighter blue arrows showing the directions of the transposase genes. ISAba1 that flanks the composite transposon is depicted in darker shades of blue. The 9-bp direct repeat sequences that flank the composite transposon are shown in red fonts. Antimicrobial resistance genes are shown as yellow arrows; brown arrows are toxin-antitoxin systems; purple arrows are putative DNA recombination genes; other colored arrows are genes with known homologs; white arrows are ORFs encoding hypothetical proteins. Gray-shaded areas indicate regions with >99% nucleotide sequence identities. The linear map of pNDM-1_AP882 covers nt 146571 to 146597 and continues with nt 1 to 14741 of accession no. CP014478, whereas the map of pAC1530 covers nt 147515 to 173972 and continues with nt 1 to 15685 of accession no. CP045561.1. Note that plasmid pAC1633-1 (accession no. CP059301) is almost identical to pAC1530 within this region except for the omission of the *relBE* toxin-antitoxin system and its downstream ORF, as detailed in the text and in Fig. 2.

sequence analysis subsequently indicated that the ISAba1-flanked composite transposon, designated Tn6948 by the Transposon Registry (48), is 14,750 bp and details of its structure and how the 42-kb region in pAC1530 (as well as pAC1633-1) came about will be presented in a later section of the manuscript.

The bla_{NDM-1} gene is found within a 10,099-bp Tn125 composite transposon that was made up of a pair of flanking ISAba125 elements and is a common genetic vehicle for the dissemination of bla_{NDM} genes in *Acinetobacter* spp. (22, 23, 49). One copy of ISAba125 is 93 bp upstream of bla_{NDM-1} and the presence of an outward-directing promoter at the terminal inverted repeat of ISAba125 likely drives the expression of bla_{NDM-1} (23, 50). In both pAC1633-1 and pAC1530, Tn125 was inserted into an unknown open reading frame, resulting in a 3-bp target site duplication ("ACG"), as has been previously reported for this transposon (23, 49, 50), although instances where a 4-bp duplication of the Tn125 site of insertion have been reported (51).

The bla_{OXA-58} and *msrE-mphE* resistance genes, and the toxin-antitoxin systems, are in p*dif* modules on pAC1633-1 and pAC1530. One of the intriguing features of *Acinetobacter* plasmids is the presence of discrete modules flanked by conserved inverted repeats homologous to the XerC and XerD binding sites (*dif* sites) separated by a 6-bp spacer, which are recombination targets for the XerC and XerD proteins (52–54). Since their initial discovery flanking a discrete module encoding the OXA-24 carbapenemase gene in the *A. baumannii* pABVA01a plasmid (55), several of these designated p*dif* modules (named for plasmid *dif*) which comprise a pair of inverted p*dif* sites surrounding a gene or several genes, have been described (54, 56). In pAC1633-1 and pAC1530, the region surrounding bla_{OXA-58} is rich in p*dif* sites; 11 of the 14 p*dif* sites in pAC1530 were located within a 14,410-bp fragment that spanned nt 153566 to 167912 (Fig. 4). The bla_{OXA-58} gene itself is flanked by IS elements (a partial 427-bp ISAba3 upstream of bla_{OXA-58} and full copies of ISAba11 and ISAba3 immediately downstream), which are in turn flanked by a pair of inverted p*dif* sites, an arrangement that has been previously reported for the *A. johnsonii*-encoded plasmid pXBB1-9, but without the presence of ISAba11 (57). In pAC1633-1/pAC1530, insertion of ISAba11 led to a characteristic 5-bp direct repeat (ATTTA) of the target sequence. In some *Acinetobacter*, a full ISAba3 or ISAba3-like element is found upstream of bla_{OXA-58}, while in other instances this upstream ISAba3 is disrupted by other IS elements (53, 58–60).
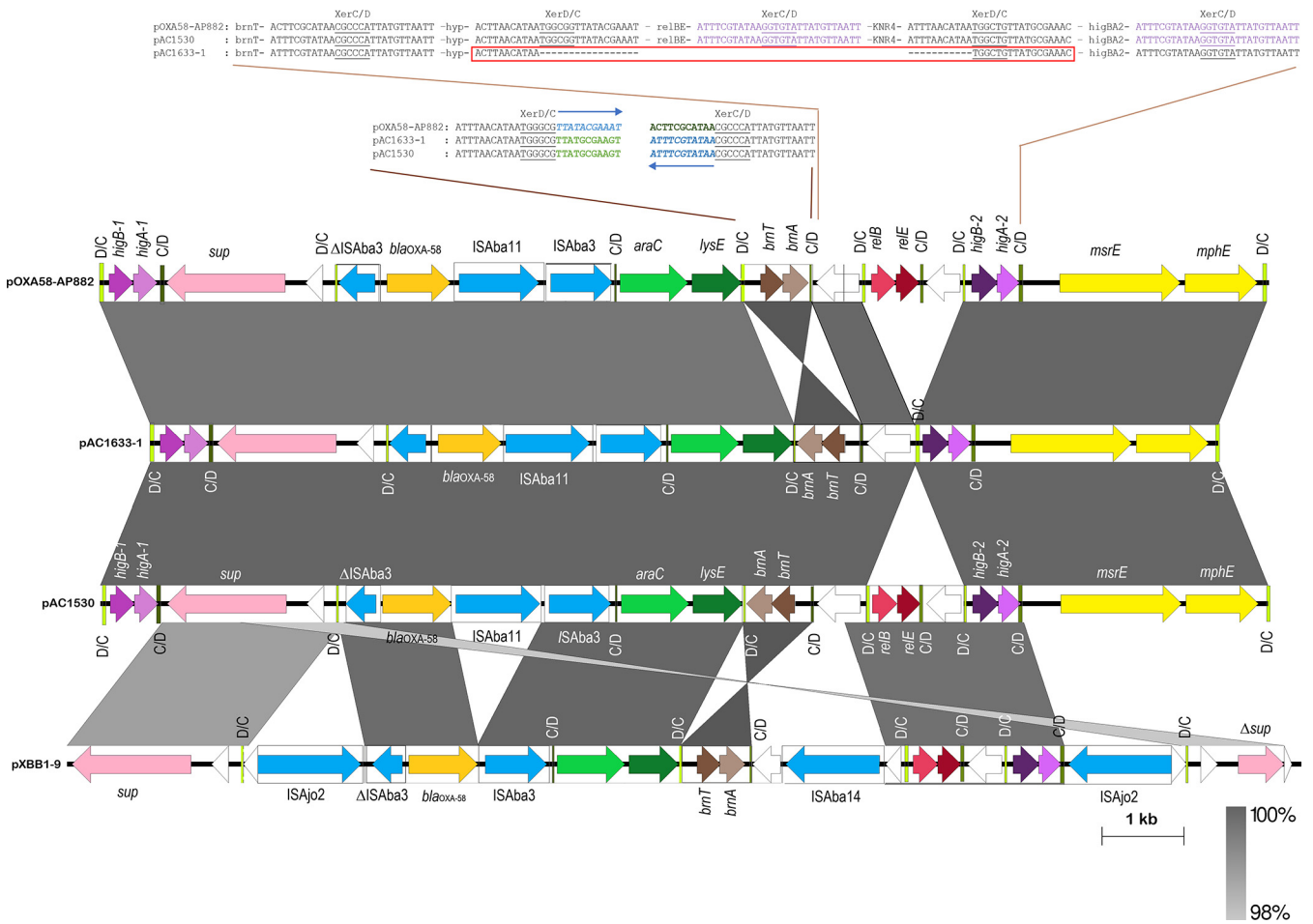
FIG 4 Comparative map of the p*dif*-rich regions surrounding the *bla*_{OXA-58} gene in several *Acinetobacter* plasmids. Arrows indicate the extents and directions of the genes and ORFs with the *bla*_{OXA-58} gene depicted as a gold arrow, the *msrE* and *mphE* macrolide resistance genes in yellow, and the aminoglycoside resistance gene *aac(3)-IId* shown in orange. IS elements are shown as boxes with their encoded transposases in blue arrows within the respective boxes. The p*dif* sites are depicted as vertical bars with the orientation of the sites labeled and colored as follows: XerD/XerC colored lime green and labeled as D/C; XerC/XerD colored dark olive green and labeled as C/D. Note the toxin-antitoxin genes that make up the following p*dif* modules: *higBA-1*, *higBA-2*, *brnTA*, and *relBE*. Other genes are labeled as follows: *araC*, putative transcriptional regulator of the AraC family; *lysE*, putative threonine efflux protein; and *sup*, putative sulfate transporter. White arrows depict ORFs that encode hypothetical proteins. The p*dif* sequences (either XerD/C or XerC/D) in pAC1633-1/pAC1530 and pOXA-58_AP882 at the inversion region encompassing *brnTA* and the insertion point of the *relBE* TA system are indicated for the respective plasmids and their relevant regions. For the *brnTA* p*dif* module, note that the XerC sequences in pOXA-58_AP882 are in reverse orientation compared to the corresponding XerC sequences in pAC1633-1 and pAC1530; these are indicated by blue arrows as well as blue and green fonts for the respective p*dif* XerC site. Also note that the p*dif* sequences downstream of the *relE* gene are identical with the p*dif* sequences downstream of the *higA-2* gene, and these sequences are in purple fonts. The p*dif* (XerD/C) site in pAC1633-1 in which the *relBE*-SMI1/KNR4 p*dif* module was inserted in pAC1530 is outlined in a red box and its sequences outlined likewise below. Note that for this particular p*dif* site, the XerD sequences are identical to the XerD sequences of the p*dif* site upstream of *relB* while the 6-bp spacer and XerC sequences are identical to the p*dif* site upstream of *higB-2*. Accession numbers and coverage of plasmid regions for the comparative map are as follows: pOXA-58_AP882 (accession no. CP014479; nt 25121 to 36862 and continued from 1 to 2560); pAC1633-1 (accession no. CP059301; nt 155106 to 168160); pAC1530 (accession no. CP045561.1; nt 153566 to 167840); pXBB1-9 (accession no. CP010351; nt 2158 to 1 and continued from nt 398857 to 398921). The extent of regions with nucleotide sequence identities of between 98 to 100% are shown in gray.

A pair of inversely oriented p*dif* sites was also found to flank the *msrE* and *mphE* macrolide resistance genes in pAC1633-1 and pAC1530 (Fig. 4), leading to the formation of a 2,950-bp macrolide-resistance p*dif* module, as had been reported previously in other *Acinetobacter* plasmids (53). This *msrE-mphE* module has always been found adjacent to a *higBA* TA p*dif* module (53), and this was also the case in pAC1633-1 and pAC1530.

Intriguingly, all known TA systems detected in pAC1633-1 and pAC1530 (*higBA-1*, *brnTA*, and *higBA-2*) were found within this region and they were each flanked by a pair of inverted p*dif* sites. As mentioned earlier, one of the differences between pAC1633-1 and pAC1530 is the addition of a *relBE* TA system and an ORF encoding a

protein of the SMI1/KNR4 family in pAC1530, upstream of *higBA-2* (Fig. 4). The *relBE* genes and the genes encoding SMI1/KNR4 protein are also p*dif* modules, as they are each flanked by a pair of inverted p*dif* sites. A closer examination of the p*dif* (XerD/C) sequences showed that in pAC1633-1, the p*dif* (XerD/C) sequences upstream of *higBA-2* are a hybrid of the p*dif* (XerD/C) sequences that flanked the *relBE*-SMI1/KNR4 module in pAC1633-1, i.e., the sequences of the XerD site are identical to the sequences found upstream of *relBE*, while the 6-bp spacer and the XerC site sequences are identical to the sequences upstream of *higBA-2* in pAC1633-1 (Fig. 4). This suggests the *relBE*-SMI1/KNR4 p*dif* module could have been deleted from pAC1530 in pAC1633-1 via a Xer-mediated recombination event.

Another Xer-related rearrangement could be seen when comparing the sequences of pAC1633-1 and pAC1530 with their closest plasmid relative, pOXA-58_AP882, wherein the *brnTA* TA p*dif* module was found to be in inverted orientation. The orientation of *brnTA* in pOXA-58_AP882 is, however, the same in pXBB1-9 (Fig. 4). Interestingly, the XerD and the 6-bp spacer sequences of the flanking p*dif* modules for *brnTA* are identical when comparing pAC1633-1/pAC1530 with pOXA-58_AP882, except the XerC sequences are inverted (pAC1633-1/pAC1530: TTATGCGAAGT; pOXA-58_AP882: ACTTCGCATAA) (Fig. 4). Currently, genome sequencing data strongly support the likelihood that p*dif* modules are mobile, although, to our knowledge, there has yet to be any definite experimental evidence offered or mechanism of mobility elucidated (52). Deletions and inversions of *Acinetobacter* p*dif* modules have been hinted at (52, 56), and here we show sequence evidence that these do occur.

pAC1633-1/pAC1530 is likely a hybrid of two plasmids with the cointegration mediated by IS*1006*. BLASTN analysis of pAC1633-1 and pAC1530 showed they are most similar in sequence to two plasmids found in *Acinetobacter pittii* AP882 designated pNDM-1_AP882 (accession no. CP014478) and pOXA-58_AP882 (accession no. CP014479). Notably, *A. pittii* AP882 was isolated from Peninsular Malaysia in 2014 but from a different state (Perak) (61) compared to AC1633-1 and AC1530 (isolated from Terengganu in 2016 and 2015, respectively). When comparing the 146,597-bp pNDM-1_AP882 with pAC1530 and pAC1633-1, pNDM-1_AP882 is nearly identical with pAC1530/pAC1633-1 except for a 1,940-bp region adjacent to IS*1006*. This region contains a 1,472-bp IS-like sequence (nt 4480 to 1472) that encodes two transposases characteristic of the IS*3* family flanked by 21/22-bp imperfect inverted repeats and a 5-bp direct repeat (ACCTG) of the target sequence (Fig. S1). Further analysis of pNDM-1_AP882 led to the discovery of a 14,750-bp composite transposon designated Tn*6948*, formed by flanking IS*Aba1* sequences with a 9-bp target site duplication (TTAAAAATT) that is characteristic of this IS element (Fig. 3). The target site duplication is only found for the entire transposon structure but not for each individual IS*Aba1* element, thus suggesting this is likely an active transposon. Tn*6948* harbors the *sul2* sulfonamide resistance gene and the aminoglycoside resistance genes *aph(3″)-Ib*, *aph(6)-Id*, and *aac(3)-IId*. Tn*6948* has an overall GC content of 50.6% compared to 38 to 39% for the surrounding genes, thus supporting its possible non-*Acinetobacter* origin.

When comparing the 36,862-bp pOXA-58_AP882 plasmid with pAC1530 and pAC1633-1, a 29,671-bp fragment of pOXA-58_AP882 was found to be identical to pAC1530/pAC1633-1, and this region, which comprises the resistance genes *bla*$_{OXA-58}$, *msrE*, *mphE*, and *adeABC-adeRS*, is flanked by two copies of IS*1006* (Fig. 5A). The remaining 7,191 bp of pOXA-58_AP882 that was absent in pAC1530/pAC1633-1 encodes 10 ORFs and this includes ORFs that encode a MobA/L mobilization protein, a Rep3 family *Acinetobacter* replicase of the GR12 group (62), a hypothetical protein with a helix-turn-helix motif that had previously been misannotated as RepA (43), a protein of the RelE/ParE toxin family and, downstream of it, an ORF that encodes another helix-turn-helix protein but of the Xre family (Fig. S1). The putative RelE/ParE family toxin in this region of pOXA-58_AP882 shared only 27% amino acid sequence identity with the RelE toxin of the previous RelBE TA pair found within this plasmid as well as in pAC1530 (but which was absent in pAC1633-1). In comparing the IS*1006* sequences in these plasmids, it was found that the two IS*1006* copies in pOXA-58_AP882 were
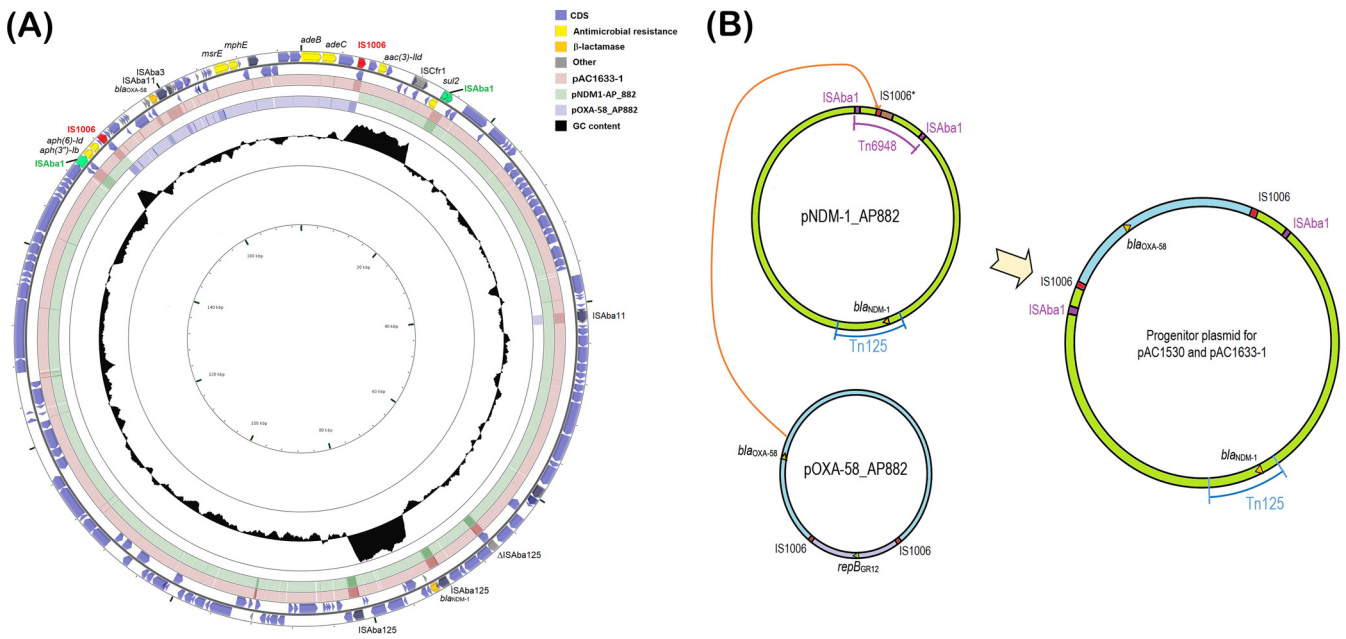
(A)

(B)

FIG 5 (A). Comparison of pAC1633-1 with plasmids pNDM-1_AP882 and pOXA-58_AP882 from *Acinetobacter pittii* strain AP882. The outer two circles show the genes and coding sequences (CDS) from pAC1633-1 with the two copies of IS*1006* marked in red and the antimicrobial resistance genes in yellow. The two IS*Aba1* elements that flank the composite transposon Tn*6948* in pNDM-1_AP882 are shown in green. The pink-colored ring indicates pAC1633-1, while the green- and blue-colored inner rings show regions of pNDM-1_AP882 and pOXA-58_AP882, respectively, that share >95% nucleotide sequence identities with the corresponding region in pAC1633-1. The inner black ring depicts a plot of the GC content of pAC16331 with the baseline set as the average GC content of 38% for the plasmid. Note the Tn*125* encoding *bla*$_{NDM-1}$ and Tn*6948* had higher GC content (~50%) than the average, with their plots extending outward from the circle. Darker shades of pink, green, and blue indicate repeat regions (usually IS elements). Note that pAC1633-1 could possibly came about through integration of the IS*1006*-flanked region that encompasses the *bla*$_{OXA-58}$, *msrE*, and *mphE* resistance genes into the single IS*1006* copy of pNDM-1_AP882, as illustrated in panel B. (B) Hypothetical IS*1006*-mediated cointegration for the generation of the predecessor plasmid for pAC1530 and pAC1633-1 from pNDM-1_AP882 and pOXA-58_AP882. The 29,671-bp region of pOXA-58_AP882 that contains the *bla*$_{OXA-58}$ gene and is flanked by IS*1006* (labeled in light blue) likely recombined with pNDM-1_AP882 at its single IS*1006* region, leading to the formation of the cointegrate predecessor plasmid for pAC1530 and pAC1633-1 that harbored both *bla*$_{OXA-58}$ and *bla*$_{NDM-1}$. The light purple region in pOXA-58_AP882 contains the *repB* replicase gene of the *Acinetobacter* GR12 family and was not involved in the plasmid cointegrate formation. IS*1006* is depicted as red boxes and labeled. pNDM-1_AP882 harbored an IS*1006* with a T175C mutation (compared with the IS*1006* sequences in pOXA-58_AP882) and is labeled as IS*1006**. The brown-colored box in pNDM-1_AP882 refers to a 1,940-bp region adjacent to IS*1006** that was absent in pAC1530 and pAC1633-1 and contained an IS*3* family element. This region could have been deleted during the IS*1006*-mediated cointegration process or after the formation of the cointegrate plasmid. The IS*Aba1* elements that flank the composite transposon Tn*6948* in pNDM-1_AP882 are indicated in purple boxes and labeled.

identical with the two copies in pAC1530 and pAC1633-1. However, the solitary IS*1006* copy in pNDM-1_AP882 had a single nucleotide change in which T replaced C at nt 175 of the 819-bp IS*1006*.

It is thus tempting to speculate that the 29,671-bp region of pOXA-58_AP882 that contained *bla*$_{OXA-58}$ formed a composite transposon-like structure flanked by two copies of IS*1006* and that this region could have transposed or recombined with pNDM-1_AP882 at its single IS*1006* copy residing within Tn*6948*. This transposition or recombination might have resulted in a predecessor for plasmids pAC1530 and pAC1633-1, which contain both the *bla*$_{NDM-1}$ and *bla*$_{OXA-58}$ genes in a single plasmid that has two copies of IS*1006* (Fig. 5B). IS*1006* belongs to the large IS*6*/IS*26* family of IS elements (63) and this family, in particular IS*26*, has been known to mediate the formation of cointegrates between two DNA molecules, with the donor molecule harboring IS*26* (64). However, this route, designated "replicative" or "copy-in," usually leads to the formation of an 8-bp target site duplication for the IS*26* and inserts at random sites (63). Here, no target site duplication could be detected in pAC1530, pAC1633-1, or even pOXA-58_AP882 at the ends of the IS*1006*-flanked region. Nevertheless, IS*26* was recently demonstrated to perform a unique transposase-dependent reaction when both donor and target molecules carry a copy of IS*26*. This reaction, designated "targeted conservative," is targeted, occurring at one or the other end of the two IS*26* elements, and with the IS element not duplicated and a target site duplication not generated (65). Cointegration by the targeted conservative route was found to

TABLE 4 Conjugative transfer-related genes identified in pAC1530 and pAC1633-1 compared to their corresponding genes in pA297-3

Gene	Product size pAC1530[a] (aa)	Product size pA297-3[b] (aa)	% Protein identity[d]	Possible function[c]
Region 1				
traW	378	377	75 (282/376)	Lipoprotein
traY	902	882	66 (526/729)	Integral membrane protein
trbA	445	456	62 (273/443)	Formation of thick pilus/ DNA transfer
traJ	408	429	62 (262/410)	DNA-binding protein
traI	277	272	69 (192/279)	Lipoprotein
traH	156	156	66 (105/158)	Lipoprotein
traM	232	238	60 (133/231)	Formation of thick pilus/ DNA transfer
traN	367	376	63 (237/379)	Signal peptide
traO	541	543	50 (252/501)	Formation of thick pilus/ DNA transfer
icmJ[e]	255	252	60 (149/250)	
traU	1088	1090	70 (754/1084)	Nucleotide-binding protein
trbC	913	912	61 (569/912)	Nucleotide-binding protein
Region 2				
traC	632	616	49 (305/619)	Inner membrane complex ATPase
trbN[f]	272	275	50 (142/266)	Major pilus subunit
traB	750	753	60 (451/753)	Outer membrane complex

[a]GenBank accession no. CP045561.1.
[b]GenBank accession no. KU744946.1 (Hamidian et al., 2016) (67).
[c]Predicted function as listed in Hamidian et al. (2016) (67) and Christie (2016) (91).
[d]Numbers in parentheses indicate amino acid identities.
[e]icmJ as annotated by PROKKA; shared 60% amino acid sequence identity with HPG66_RS00900 of pA297-3, which was annotated as hypothetical; low sequence identities (42%; 18/43) with IcmJ of *Legionella pneumophila* (accession no. CAH11669.1).
[f]trbN was annotated by Hamidian et al. (2016) (67) for pA297-3 and pD46-4 (Nigro and Hall, 2017) (70); no detectable similarities with other conjugal proteins.

be the preferred reaction if two copies of IS*26* in two different DNA molecules are available (65, 66). Based on sequence analysis alone, it is difficult to ascertain the mechanism by which the predecessor cointegrate plasmid for pAC1530 and pAC1633-1 was formed, i.e., whether it was through the targeted conservative route since both pOXA-58_AP882 and pNDM-1_AP882 harbored IS*1006*, or by homologous recombination via IS*1006*, or even by classical transposition—as the two copies of IS*1006* that flanked the 29,671-bp bla_{OXA-58} fragment do form a composite transposon structure, albeit without the characteristic target site duplications at its termini.

Transmissibility of pAC1530 and pAC1633-1. The fact that pAC1530 and pAC1633-1 were nearly identical, large (>170 kb) plasmids that were isolated from two different *Acinetobacter* species in two different years (*A. nosocomialis* AC1530 from 2015 and *A. baumannii* AC1633 from 2016) but from the same hospital is suggestive of plasmid transmissibility. Sequence analysis also indicated the presence of several conjugative transfer-related genes, most of which share between 50 to 70% amino acid sequence identities with the corresponding translated proteins of the conjugative plasmid pA297-3 from *A. baumannii* isolate A297 (67) (Table 4). The conjugative transfer genes of pAC1530 and pAC1633-1 were broadly distributed in two large regions of the plasmids, as they were in pA297-3. The order of the transfer genes in both regions in pAC1530 and pAC1633-1 (designated regions 1 and 2) was identical with the order in pA297-3, despite that the nucleotide sequence identities were lower than 65% in some parts of these two regions (Fig. 6). However, in both pAC1530 and pAC1633-1, region
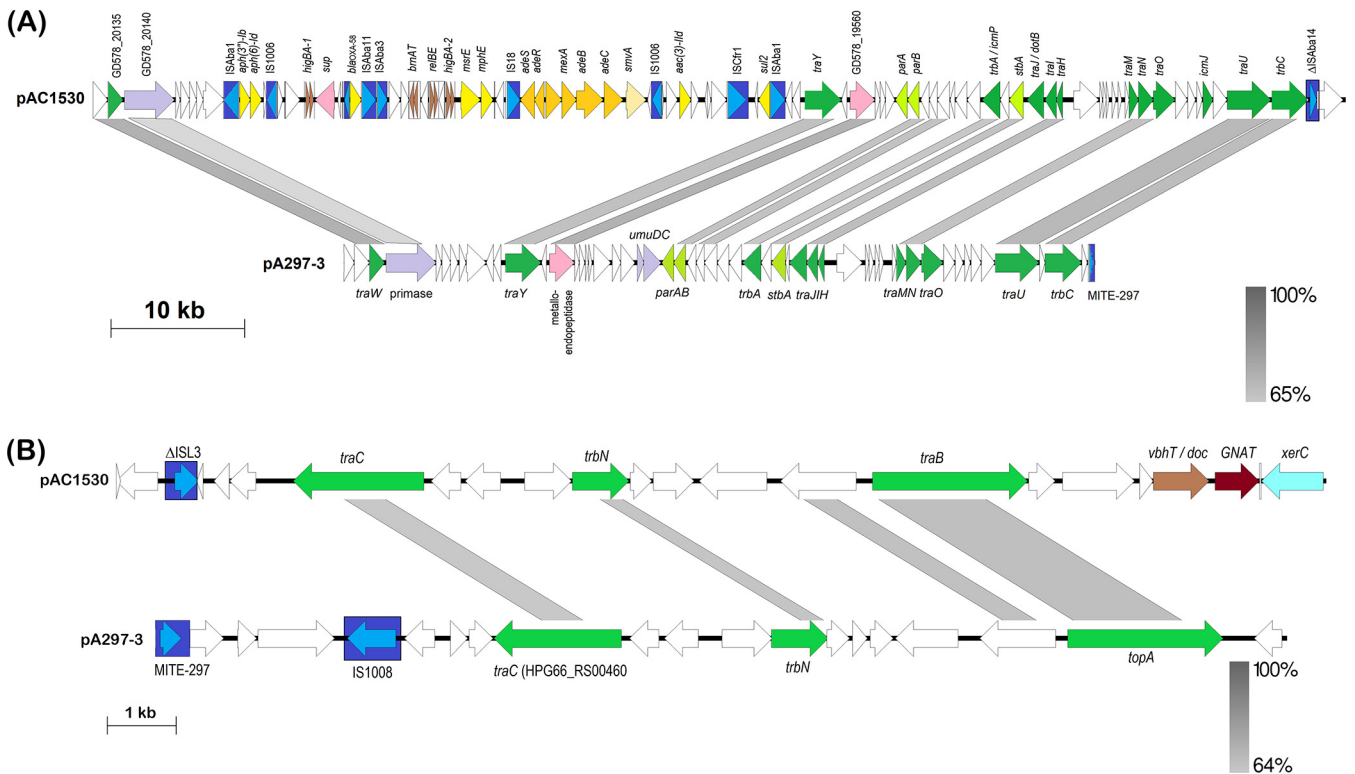
FIG 6 Linearized map of the two conjugative regions of pAC1530 compared to pA297-3. (A) Region 1; map shows nt 137720 to 173972 and continues with 1 to 57600 of pAC1530 (numbered as in accession no. CP045561.1) and the reverse complement of nt 169947 to 200633, continues with 1 to 25440 of pA297-3 (numbered as in accession no. KU744946.1). (B) Region 2; map depicts nt 80481 to 98080 of pAC1530 and the reverse complement of nt 76001 to 92455 of pA297-3. Arrows indicate the extents and directions of genes and ORFs with identified conjugative transfer genes depicted as dark green arrows. Lime green arrows are the plasmid partitioning genes *parA* and *parB*. IS elements and the miniature inverted-repeat transposable element (MITE) identified in pA297-3 (67) are depicted as dark blue boxes with their encoded transposase shown as lighter blue arrows. Antibiotic resistance genes in pAC1530 are indicated as yellow arrows while toxin-antitoxin genes are shown as brown arrows. Other identified genes are in purple and pink arrows, with white arrows indicating ORFs encoding hypothetical proteins. The IS*Aba1*-flanked Tn*6948* is indicated; note that in pAC1530 and pAC1633-1, Tn*6948* is interrupted by the IS*1006*-flanked region that contains antimicrobial resistance genes such as *bla*$_{OXA-58}$, *sul2*, *msrE*, and *mphE* (see Fig. 3 and text). Gray-shaded areas indicate regions with DNA sequence identities as indicated by the bars at the bottom right of each figure. Note that although the figure depicts only pAC1530, pAC1633-1 is nearly identical to pAC1530 in Region 1 except for an insertion of IS*Aba11* in the ORF upstream of *traM* and deletion of the *relBE* p*dif* module (see Fig. 2 and text).

1, which spans from *traW* to *trbC*, was interrupted by a 42-kb fragment encompassing the IS*Aba1*-flanked composite transposon Tn*6948* and, nested within it, the 29-kb IS*1006*-flanked fragment derived from pOXA-58_AP882 (Fig. 6). Conjugation assays were performed using the carbapenem resistant parental hosts, *A. baumannii* AC1633 and *A. nosocomialis* AC1530, as donor strains and, as recipients, carbapenem suscepti-ble *A. baumannii* ATCC 19606 and *A. baumannii* AC1529 clinical isolate that were induced to sodium azide resistance with MIC values of >300 μg/ml. Despite repeated attempts with established conjugation assay protocols (67, 68) and using different ratios of donor to recipient cells, no transconjugants were obtained that were able to grow on the selection plates (LB agar supplemented with 10 μg/ml imipenem and 300 μg/ml sodium azide). Thus, we were unable to provide direct laboratory experi-mental evidence that pAC1530 and pAC1633-1 were transmissible. The 200-kb pA297-3 plasmid from *A. baumannii* A297, which encodes the *sul2* sulfonamide and *strAB* streptomycin resistance genes, was found to transfer sulfonamide and streptomycin re-sistance to a rifampin-resistant *A. baumannii* ATCC 17974 strain at a high frequency of 7.20×10^{-2} transconjugants/donor (67). However, two other plasmids, pD4 and pD46-4, which shared the transfer regions with pA297-3, were found to be nontransmissible (69, 70). In the case of pD4, an IS*Aba25*-like element was inserted into the DNA primase gene downstream of *traW*, indicating the possibility that this gene could be involved in conjugative transfer (69). However, for pD46-4, no such IS or other genetic elements were found to have interrupted the conjugative transfer-related genes. Also, no SNPs

were detected in the transfer genes that might have led to a frameshift or a premature stop codon within these genes (70). The reason for the apparent nontransmissibility of pD46-4 compared to pA297-3 was not known (70). As for pAC1530 and pAC1633-1, their apparent nontransmissibility could be attributed to the insertion of the 42-kb fragment containing Tn*6948* and the IS*1006*-flanked resistance region from pOXA-58_AP882 into the conjugative transfer region 1. However, the insertion of Tn*6948* at the same site was already present in pNDM-1_AP882, although, here the insertion was only 14.2 kb (Fig. 3). There was also no experimental evidence of the transmissibility of pNDM-1_AP882, although in this case the recipient strain used was an azide-resistant derivative of *E. coli* J53 (61). Nevertheless, the genomic sequence evidence presented here strongly infers the transmissible nature of pNDM-1_AP882 and, by extension, pAC1530 and pAC1633-1, as these three highly related plasmids were found in three different species of *Acinetobacter*. Perhaps the rate of conjugative transfer for these plasmids was exceptionally low and thus below detectable limits, in stark contrast to what was reported for pA297-3 in which the conjugative transfer region 1 was uninterrupted. Alternatively, successful conjugative transfer of these plasmids may require certain environmental or media conditions that were not met when the experiments were conducted in the laboratory using established protocols. Further work is clearly needed to resolve this transmissibility conundrum for pAC1530 and pAC1633-1.
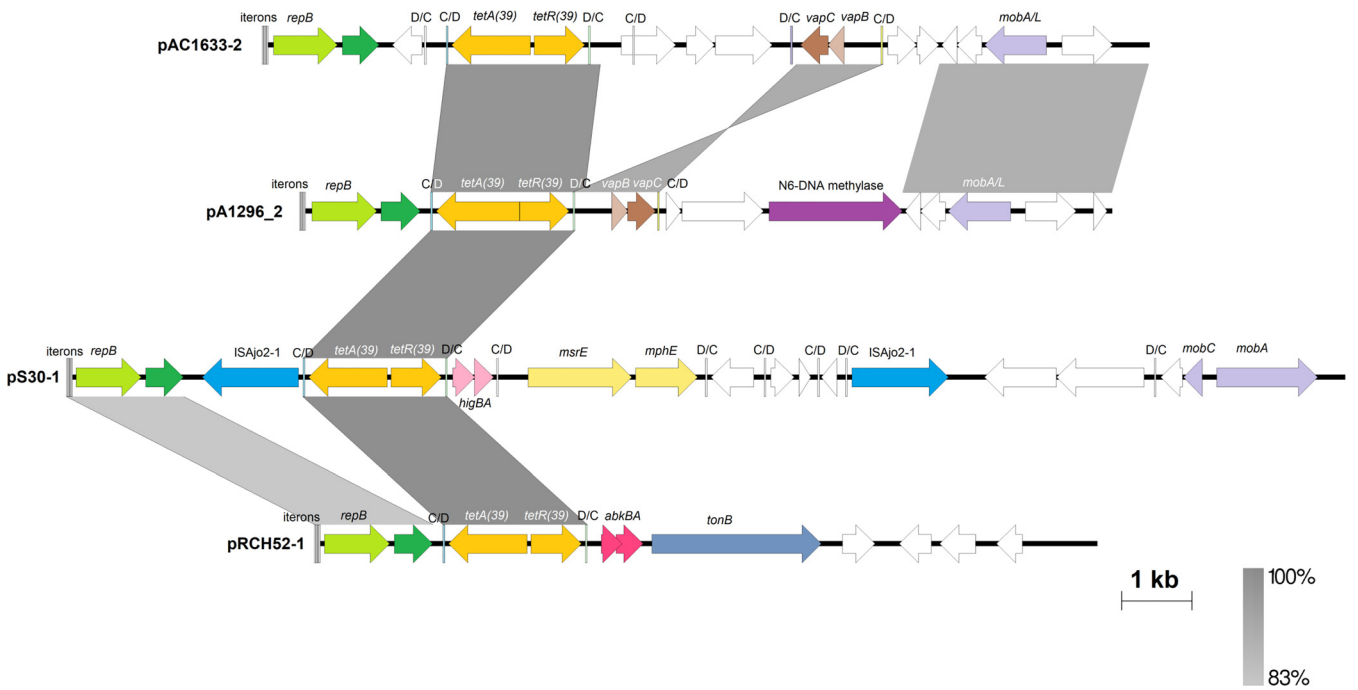
The *tetA*(*39*) tetracycline resistance gene in pAC1633-2 is within a p*dif* module. Plasmid pAC1633-2 is 12,651 bp and encodes a Rep3 family replicase of the *Acinetobacter* GR8/GR23 group that was preceded by four 22-bp iterons characteristic of Rep3 family plasmids (42, 43). pAC1633-2 also encodes a *tetA*(*39*) tetracycline resistance gene which was adjacent to and divergently transcribed from a *tetR*(*39*) regulatory gene (Fig. 7). This 2,001-bp fragment is identical with the *tetAR*(*39*) genes that made up a p*dif* module in plasmids pS30-1, pRCH52-1, and pAB1-H8 (53). However, the p*dif* sites that flank this *tetAR*(*39*) region in pAC1633-2 differed from those in pS30-1, pRCH52-1, and pAB1-H8 at the 6-bp spacer and the XerC-recognition site (Fig. 7). Another p*dif* module that was detected in pAC1633-2 encodes the *vapBC* toxin-antitoxin system, which was in an inverted orientation compared with plasmid pA1296_2 from *A. baumannii* A1296 (accession no. CP018334) (Fig. 7).

AC1633-2 also harbors a *mobA/L* gene that encodes a relaxase of the MOB$_Q$ family, indicating the possibility of the plasmid being mobilized should a suitable conjugative plasmid be present in the host cell. Since AC1633 also harbored the potentially conjugative pAC1633-1 plasmid, the ability of pAC1633-1 to mobilize pAC1633-2 was tested in conjugation experiments by selecting for transconjugants that exhibit tetracycline resistance in addition to azide resistance. Despite repeated experiments, no such transconjugants were detected, indicating that pAC1633-1 was unable to mobilize pAC1633-2. This, however, does not rule out the possibility that pAC1633-2 could be mobilized by a different type of conjugative plasmid to pAC1633-1.

Two other plasmids in *A. baumannii* AC1633, pAC1633-3 and pAC1633-4, are cryptic. Two other smaller plasmids are found in *A. baumannii* AC1633, the 9,950-bp pAC1633-3 and the 5,210-bp pAC1633-4. Neither plasmid carries any antimicrobial or metal resistance genes, nor any genes that could confer a specific phenotype to their host, and are thus characterized as cryptic plasmids. Both plasmids encode replicases of the Rep3 superfamily that are common in *Acinetobacter* plasmids, with pAC1633-3 belonging to the GR28 group where pAC1633-4 belongs to the GR7 group (42, 43). pAC1633-3 and pAC1633-4 could potentially be mobilizable, as they carry *mobA/L* genes of the MOB$_Q$ family and pAC1633-4 also carries a *mobS*-like gene. However, in the absence of any selectable marker, we were unable to determine if these two plasmids could be mobilized by pAC1633-1.

Four p*dif* sites were detected in pAC1633-3 but none in pAC1633-4. Interestingly, one of the p*dif* modules in pAC1633-3 is 464 bp, encodes a putative protein of the SMI1/KNR4 family, and is identical with the p*dif* module that was found downstream of the *relBE* p*dif* module in the *A. nosocomialis* AC1530-derived pAC1530. This SMI1/KNR4

FIG 7 Linearized map of pAC1633-2 compared to other similar plasmids harboring the *tetAR*(*39*) p*dif* module. Arrows indicate the extents and directions of genes and ORFs with yellow arrows for the *tetA*(*39*) and *tetR*(*39*) tetracycline resistance genes and pale yellow arrows for the macrolide resistance genes *msrE* and *mphE* in pS30-1. Plasmid replicase genes of the Rep3 family are depicted as green arrows and labeled *repB*, while darker green arrows are ORFs encoding putative DNA-binding proteins that have been previously misannotated as *repA* (43). Mobilization-related genes are shown as light purple arrows and the gene encoding an N6-DNA methylase is in dark purple. The *vapBC* toxin-antitoxin genes in pAC1633-2 and pA1296_2 are indicated as brown arrows; *higBA* in pS30-1 are depicted in pink; whereas *abkBA* in pRCH52-1 are in dark pink. The transposase encoded by ISAjo2 in pS30-1 is colored blue. White arrows are ORFs that encode hypothetical proteins. Regions with significant DNA identities from 83 to 100% are shaded in shades of gray as indicated in the bar at the bottom right of the figure. The four 22-bp iterons that are the likely *oriV* site for each plasmid is shown as successive horizontal bars at the beginning of the plasmid linear maps. The p*dif* sites are depicted as horizontal bars labeled as C/D for the XerC-XerD orientation and D/C for XerD-XerC orientation. Note that the orientation of the *vapBC* genes flanked by p*dif* sites in pAC1633-2 are inverted compared to pA1296_2. The XerC/D and XerD/C sites flanking the *tetAR*(*39*) genes are colored light blue and light green, respectively, whereas the XerC/D and XerD/C sites flanking the *vapBC* genes in pAC1633-2 are colored light yellow and light purple, respectively. The sequences for the p*dif* sites flanking the *tetAR*(*39*) genes as well as the *vapBC* TA genes are shown in the table at the bottom of the figure. Bases highlighted in red are those that differ from the p*dif* sequences of pAC1633-2. The accession numbers of the plasmids used in this analysis are as follows: pA1296_2 (accession no. CP018334), pS30-1 (accession no. KY617771), and pRCH52-1 (accession no. KT346360).

p*dif* module, along with the *relBE* p*dif* module, is absent in pAC1633-1 and is one of the features that differentiates pAC1530 from pAC1633-1. The other p*dif* module in pAC1633-3 is 4,331 bp and encodes a putative regulatory protein of the Xre family, a *hipA*-like toxin, and a 602-amino acid protein of the DEAD/DEAH box family of helicases.

In summary, complete genome sequencing of carbapenem-resistant *A. baumannii* AC1633 and *A. nosocomialis* AC1530 isolates led to the discovery of a ca. 170-kb plasmid that encodes the NDM-1 and OXA-58 carbapenemases along with several other resistance determinants and was likely responsible for the MDR status of these two clinical isolates. The *A. baumannii* AC1633-derived pAC1633-1 and the *A. nosocomialis* AC1530-derived pAC1530 were nearly identical except for the insertion and deletion of IS elements and a p*dif* module. Both plasmids were a patchwork of multiple mobile genetic elements, with the *bla*$_{NDM-1}$ gene residing in a Tn*125* composite transposon while *bla*$_{OXA-58}$ was flanked by IS elements nested within a p*dif* module. The *msrE-mphE*

macrolide resistance genes were also located within a p*dif* module, as were several toxin-antitoxin genes, highlighting the importance of these Xer recombination-dependent modules as one of the drivers of plasmid diversity in *Acinetobacter*. Comparative sequence analysis indicated that pAC1633-1/pAC1530 is likely a cointegrate of two plasmids which separately encode the bla_{NDM-1} and bla_{OXA-58} genes in an *A. pittii* clinical isolate, and that was formed via an IS*1006*-mediated recombination or transposition event. Horizontal transmission of pAC1633-1/pAC1530 was inferred from the discovery of the almost identical plasmid in two different species of *Acinetobacter* from the same hospital, though this could not be experimentally replicated in the laboratory. Nevertheless, the presence of such large, potentially transmissible multidrug resistance plasmids in *Acinetobacter* that coharbor the NDM-1 and OXA-58 carbapenemases in this and other recent reports (51, 57) warrants monitoring and assessment of the risk of spread of these plasmids to susceptible strains, particularly in healthcare settings.

MATERIALS AND METHODS

Ethical approval, bacterial isolates, and antimicrobial susceptibility profiles. Ethical approval for this study was obtained from the Malaysian Ministry of Health's National Medical Research Register (approval no. NMRR-14-1650-23625-IIR). *A. baumannii* AC1633 and *A. nosocomialis* AC1530 were isolated from Hospital Sultanah Nur Zahirah, Kuala Terengganu, Malaysia in 2016 and 2015, respectively. Species identification of both isolates was performed by sequencing of the *rpoB* gene as previously described (13, 71). Antimicrobial susceptibility profiles of both isolates were determined using a panel of 22 antibiotics recommended for *Acinetobacter* spp. (26) and by disk diffusion (Oxoid Ltd., Basingstoke, UK) on Mueller-Hinton (MH) agar, except for colistin and polymyxin B, which were determined by obtaining the MIC values by the agar diffusion method (25). Carbapenem resistance was validated by determining the MIC values for imipenem, meropenem and doripenem using M.I.C. Evaluator strips (Oxoid Ltd., Basingstoke, UK). Results were interpreted according to the Clinical and Laboratory Standards Institute (CLSI) guidelines (72). Production of metalo-β-lactamases was determined using the Etest MBL kit (bioMérieux, La Balme-les-Grottes, France).

DNA isolation, whole-genome sequencing, and sequence analyses. Genomic DNA for whole-genome sequencing was prepared using the Geneaid Presto mini gDNA bacteria kit (Geneaid, Taipeh, Taiwan) following the manufacturer's recommended protocol and the extracted DNA quality was evaluated using a Qubit 2.0 fluorometer (Life Technologies, Carlsbad, CA). Genome sequencing was performed on the Illumina NextSeq (Illumina Inc., San Diego, CA) and PacBio RSII (PacBio, Menlo Park, CA) platforms by a commercial service provider (Novogene, Beijing, China) and hybrid assembly was carried out using SPAdes (version 3.11.1) (73). Gene prediction for the assembled genomes was performed with PROKKA (74) with annotation achieved using the NCBI Prokaryotic Genome Annotation Pipeline (PGAP) (75). Multilocus sequence typing (MLST) in the Institut Pasteur (76) and Oxford (77) schemes was performed via the *A. baumannii* MLST database (https://pubmlst.org/abaumannii/) (33). Pan genome analysis for *A. baumannii* AC1633, *A. nosocomialis* AC1530, and related global *A. baumannii* and *A. nosocomialis* isolates (as listed in Table S1) was determined using ROARY, with the core genomes identified using the criteria of amino acid sequence identities of >95% (78) and presence in 99% of genomes. The derived core genome alignments for *A. baumannii* and *A. nosocomialis* were then used to infer maximum-likelihood (ML) trees using FastTree (79) with 100 bootstraps under the GTR time-reversible model. The resulting *A. baumannii* and *A. nosocomialis* phylogenetic trees were then visualized using iTOL v5 (https://itol.embl.de/) (80). The *A. baumannii* and *A. nosocomialis* genomes chosen for analyses were reference genomes that were either complete and/or have been published. For *A. baumannii*, unpublished genomes of isolates originating from Malaysia were also included in the analyses.

Antibiotic resistance genes were identified using ResFinder (https://cge.cbs.dtu.dk/services/ResFinder/) (81) and the Comprehensive Antibiotic Resistance Database (CARD) (https://card.mcmaster.ca/) (82), whereas ISFinder (https://isfinder.biotoul.fr/) (41) was used to identify insertion sequences. Toxin-antitoxin systems were identified using the toxin-antitoxin database TADB 2.0 (https://bioinfo-mml.sjtu.edu.cn/TADB2/index.php) (83), and putative conjugative transfer genes were identified using SeCReT4 (https://db-mml.sjtu.edu.cn/SecReT4/) (84). All plasmid sequences were manually inspected using BLAST (https://blast.ncbi.nlm.nih.gov/Blast.cgi) and ORF Finder (https://www.ncbi.nlm.nih.gov/orffinder/) to validate the genes/open reading frames (ORFs) that were predicted by the annotation and other programs. Pfam searches (85) and the NCBI Conserved Domain Database (CDD) (86) were also used to identify possible protein functions. Plasmids similar to pAC1530 and pAC1633-1 were searched by BLASTN (at https://blast.ncbi.nlm.nih.gov/Blast.cgi) using the nonredundant (nr) nucleotide collection and initially optimized for highly similar sequences (MegaBLAST). Regions of high sequence identities with multiple hits (such as the bla_{NDM-1}-encoded Tn*125*) were then subsequently omitted from subsequent searches, which were optimized for more dissimilar sequences (discontiguous MegaBLAST) and somewhat similar sequences (BLASTN). The presence of p*dif* sites in pAC1530, pAC1633-1, and related plasmids was determined by BLASTN screening using known XerC/XerD and XerD/XerC sites in published reports (52–54) and manually examining hits that were 75 to 80% identical in sequence (54).

SnapGene 5.1.5 (GSL Biotech LLC., San Diego, CA) was used to visualize and manipulate the

sequences studied. Figures were drawn to scale using EasyFig 2.2.3 (http://mjsull.github.io/Easyfig/) (87) and CGView (http://stothard.afns.ualberta.ca/cgview_server/) (88).

Conjugation assays. Conjugation assays were carried out to investigate the transmissibility of pAC1530 and pAC1633-1 from their respective carbapenem-resistant natural hosts, *A. nosocomialis* AC1530 and *A. baumannii* AC1633, to the appropriate susceptible isolates, *A. baumannii* ATCC 19606 and *A. baumannii* AC1529. *A. baumannii* ATCC 19606 is the type strain of *A. baumannii* that has been widely used in various studies, is resistant to sulfonamides due to the presence of the *sul2* gene in its chromosome, but remains susceptible to a wide range of other antibiotics (45, 89), including the carbapenems. *A. baumannii* AC1529 was isolated from the blood of a 59-year-old male patient in the emergency ward of Hospital Sultanah Nur Zahirah in 2015 and its identity was confirmed by *rpoB* sequencing (71). AC1529 showed intermediate resistance to cefotaxime and ceftriaxone but was susceptible to the other 20 antimicrobials that were tested, including carbapenems. *A. baumannii* ATCC 19606 and *A. baumannii* AC1529 were selected for induction to azide resistance to be used as recipient strains in the conjugation assays. Spontaneous mutation of both *A. baumannii* strains to sodium azide resistance was performed by continuous exposure to increasing concentrations of sodium azide, as described by Leungtongkam et al. (90).

A. baumannii ATCC 19606 and *A. baumannii* AC1529 isolates with sodium azide MIC values of >300 μg/ml were used as recipients, whereas *A. baumannii* AC1633 and *A. nosocomialis* AC1530 were used as donors in four separate conjugation experiments. Equal amounts of overnight cultures of the donor and recipient cells were mixed and incubated at 37°C on Luria-Bertani (LB) agar plates overnight. Cells were resuspended and diluted in 0.9% NaCl and selected on LB agar plates supplemented with 300 μg/ml sodium azide and 10 μg/ml imipenem. Conjugation assays were also repeated with different ratios of donor to recipient cells (1:2, 1:3, 2:1, and 3:1). To investigate if the *tetA(39)*-harboring plasmid pAC1633-2 could be mobilized by pAC1633-1 in *A. baumannii* AC1633, conjugation experiments involving AC1633 as donor were also plated on LB agar plates supplemented with 300 μg/ml sodium azide and 4 μg/ml tetracycline.

Data availability. The complete sequence of the *A. baumannii* AC1633 chromosome was deposited in GenBank under accession no. CP059300, whereas its four plasmids were deposited under the following accession numbers: pAC1633-1 (CP059301), pAC1633-2 (CP059303), pAC1633-3 (CP059304), and pAC1633-4 (CP059302). The *A. nosocomialis* AC1530 chromosomal sequence was deposited under accession no. CP045560.1, whereas its plasmid pAC1530 was deposited under accession no. CP045561.1.

SUPPLEMENTAL MATERIAL

Supplemental material is available online only.
FIG S1, TIF file, 2.8 MB.
TABLE S1, DOCX file, 0.1 MB.

REFERENCES

1. Peleg AY, Seifert H, Paterson DL. 2008. Acinetobacter baumannii: emergence of a successful pathogen. Clin Microbiol Rev 21:538–582. https://doi.org/10.1128/CMR.00058-07.
2. Antunes LCS, Visca P, Towner KJ. 2014. Acinetobacter baumannii: evolution of a global pathogen. Pathog Dis 71:292–301. https://doi.org/10.1111/2049-632X.12125.
3. Hamidian M, Nigro SJ. 2019. Emergence, molecular mechanisms and global spread of carbapenem-resistant Acinetobacter baumannii. Microb Genom 5:e000306. https://doi.org/10.1099/mgen.0.000306.
4. Partridge SR, Kwong SM, Firth N, Jensen SO. 2018. Mobile genetic elements associated with antimicrobial resistance. Clin Microbiol Rev 31:e00088-17. https://doi.org/10.1128/CMR.00088-17.
5. Isler B, Doi Y, Bonomo RA, Paterson DL. 2018. New treatment options against carbapenem-resistant Acinetobacter baumannii infections. Antimicrob Agents Chemother 63:e01110-18. https://doi.org/10.1128/AAC.01110-18.
6. Bueno MS, Freire MP, Cunha MPV, de Barcellos TAF, Bertani A. M d J, Dos Santos CA, Chimara E, Nagamori FO, Takagi EH, Costa SF, Ito R. K d L, Abdala E, de Carvalho E, Tiba-Casas MR, Camargo CH. 2020. Detection of

pandrug-resistant ST15 Acinetobacter baumannii causing bloodstream infection in an HSCT patient in Brazil. J Antimicrob Chemother 75:2691–2693. https://doi.org/10.1093/jac/dkaa218.
7. Goic-Barisic I, Seruga Music M, Kovacic A, Tonkic M, Hrenovic J. 2017. Pan drug-resistant environmental isolate of Acinetobacter baumannii from Croatia. Microb Drug Resist 23:494–496. https://doi.org/10.1089/mdr.2016.0229.
8. Karakonstantis S, Kritsotakis EI, Gikas A. 2020. Pandrug-resistant Gram-negative bacteria: a systematic review of current epidemiology, prognosis and treatment options. J Antimicrob Chemother 75:271–282. https://doi.org/10.1093/jac/dkz401.
9. Centers for Disease Control. 2019. Antibiotic resistance threats in the United States, 2019. Centers for Disease Control and Prevention, U.S. Department of Health and Human Services, Atlanta, GA.
10. Tacconelli E, Carrara E, Savoldi A, Harbarth S, Mendelson M, Monnet DL, Pulcini C, Kahlmeter G, Kluytmans J, Carmeli Y, Ouellette M, Outterson K, Patel J, Cavaleri M, Cox EM, Houchens CR, Grayson ML, Hansen P, Singh N, Theuretzbacher U, Magrini N, WHO Pathogens Priority List Working Group. 2018. Discovery, research, and development of new antibiotics: the

WHO priority list of antibiotic-resistant bacteria and tuberculosis. Lancet Infect Dis 18:318–327. https://doi.org/10.1016/S1473-3099(17)30753-3.

11. Visca P, Seifert H, Towner KJ. 2011. Acinetobacter infection—an emerging threat to human health. IUBMB Life 63:1048–1054. https://doi.org/10.1002/iub.534.

12. Nemec A, Krizova L, Maixnerova M, van der Reijden TJK, Deschaght P, Passet V, Vaneechoutte M, Brisse S, Dijkshoorn L. 2011. Genotypic and phenotypic characterization of the Acinetobacter calcoaceticus-Acinetobacter baumannii complex with the proposal of Acinetobacter pittii sp. nov. (formerly Acinetobacter genomic species 3) and Acinetobacter nosocomialis sp. nov. (formerly Ac. Res Microbiol 162:393–404. https://doi.org/10.1016/j.resmic.2011.02.006.

13. Mohd Rani F, A Rahman NI, Ismail S, Abdullah FH, Othman N, Alattraqchi AG, Cleary DW, Clarke SC, Yeo CC. 2018. Prevalence and antimicrobial susceptibilities of Acinetobacter baumannii and non-baumannii Acinetobacters from Terengganu, Malaysia and their carriage of carbapenemase genes. J Med Microbiol 67:1538–1543. https://doi.org/10.1099/jmm.0.000844.

14. Chen F-J, Huang W-C, Liao Y-C, Wang H-Y, Lai J-F, Kuo S-C, Lauderdale T-L, Sytwu H-K. 2019. Molecular epidemiology of emerging carbapenem resistance in Acinetobacter nosocomialis and Acinetobacter pittii in Taiwan, 2010 to 2014. Antimicrob Agents Chemother 63:e02007-18. https://doi.org/10.1128/AAC.02007-18.

15. De Oliveira DMP, Forde BM, Kidd TJ, Harris PNA, Schembri MA, Beatson SA, Paterson DL, Walker MJ. 2020. Antimicrobial Resistance in ESKAPE Pathogens. Clin Microbiol Rev 33:e00181-19. https://doi.org/10.1128/CMR.00181-19.

16. Ramirez MS, Bonomo RA, Tolmasky ME. 2020. Carbapenemases: transforming Acinetobacter baumannii into a yet more dangerous menace. Biomolecules 10:720. https://doi.org/10.3390/biom10050720.

17. Evans BA, Amyes SGB. 2014. OXA β-lactamases. Clin Microbiol Rev 27:241–263. https://doi.org/10.1128/CMR.00117-13.

18. Turton JF, Ward ME, Woodford N, Kaufmann ME, Pike R, Livermore DM, Pitt TL. 2006. The role of ISAba1 in expression of OXA carbapenemase genes in Acinetobacter baumannii. FEMS Microbiol Lett 258:72–77. https://doi.org/10.1111/j.1574-6968.2006.00195.x.

19. Nigro SJ, Hall RM. 2018. Does the intrinsic oxaAb (bla OXA-51-like) gene of Acinetobacter baumannii confer resistance to carbapenems when activated by ISAba1? J Antimicrob Chemother 73:3518–3520. https://doi.org/10.1093/jac/dky334.

20. Karthikeyan K, Thirunarayan MA, Krishnan P. 2010. Coexistence of blaOXA-23 with blaNDM-1 and armA in clinical isolates of Acinetobacter baumannii from India. J Antimicrob Chemother 65:2253–2254. https://doi.org/10.1093/jac/dkq273.

21. Chen Y, Zhou Z, Jiang Y, Yu Y. 2011. Emergence of NDM-1-producing Acinetobacter baumannii in China. J Antimicrob Chemother 66:1255–1259. https://doi.org/10.1093/jac/dkr082.

22. Khan AU, Maryam L, Zarrilli R. 2017. Structure, genetics and worldwide spread of New Delhi metallo-β-lactamase (NDM): a threat to public health. BMC Microbiol 17:101. https://doi.org/10.1186/s12866-017-1012-8.

23. Bonnin RA, Poirel L, Nordmann P. 2014. New Delhi metallo-β-lactamase-producing Acinetobacter baumannii: a novel paradigm for spreading antibiotic resistance genes. Future Microbiol 9:33–41. https://doi.org/10.2217/fmb.13.69.

24. Boyd S, Livermore D, Hooper D, Hope W. 2020. Metallo-β-lactamases: structure, function, epidemiology, treatment options, and the development pipeline. Antimicrob Agents Chemother 64:e00397-20. https://doi.org/10.1128/AAC.00397-20.

25. Lean S-S, Suhaili Z, Ismail S, Rahman NIA, Othman N, Abdullah FH, Jusoh Z, Yeo CC, Thong K-L. 2014. Prevalence and genetic characterization of carbapenem- and polymyxin-resistant Acinetobacter baumannii isolated from a tertiary hospital in Terengganu, Malaysia. ISRN Microbiol 2014:953417. https://doi.org/10.1155/2014/953417.

26. Magiorakos AP, Srinivasan A, Carey RB, Carmeli Y, Falagas ME, Giske CG, Harbarth S, Hindler JF, Kahlmeter G, Olsson-Liljequist B, Paterson DL, Rice LB, Stelling J, Struelens MJ, Vatopoulos A, Weber JT, Monnet DL. 2012. Multidrug-resistant, extensively drug-resistant and pandrug-resistant bacteria: an international expert proposal for interim standard definitions for acquired resistance. Clin Microbiol Infect 18:268–281. https://doi.org/10.1111/j.1469-0691.2011.03570.x.

27. Krahn T, Wibberg D, Maus I, Winkler A, Pühler A, Poirel L, Schlüter A. 2015. Complete genome sequence of Acinetobacter baumannii CIP 70.10, a susceptible reference strain for comparative genome analyses. Genome Announc 3:e00850-15. https://doi.org/10.1128/genomeA.00850-15.

28. Mohd Rani F, Rahman NI, Ismail S, Alattraqchi AG, Cleary DW, Clarke SC, Yeo CC. 2017. Acinetobacter spp. infections in Malaysia: a review of antimicrobial resistance trends, mechanisms and epidemiology. Front Microbiol 8:2479. https://doi.org/10.3389/fmicb.2017.02479.

29. Rao M, Rashid FA, Shukor S, Hashim R, Ahmad N. 2020. Detection of antimicrobial resistance genes associated with carbapenem resistance from the whole-genome sequence of Acinetobacter baumannii isolates from Malaysia. Can J Infect Dis Med Microbiol 2020:5021064. https://doi.org/10.1155/2020/5021064.

30. Lean SS, Yeo CC, Suhaili Z, Thong KL. 2015. Whole-genome analysis of an extensively drug-resistant clinical isolate of Acinetobacter baumannii AC12: insights into the mechanisms of resistance of an ST195 clone from Malaysia. Int J Antimicrob Agents 45:178–182. https://doi.org/10.1016/j.ijantimicag.2014.10.015.

31. Lean S-S, Yeo CC, Suhaili Z, Thong K-L. 2015. Comparative genomics of two ST 195 carbapenem-resistant Acinetobacter baumannii with different susceptibility to polymyxin revealed underlying resistance mechanism. Front Microbiol 6:1445. https://doi.org/10.3389/fmicb.2015.01445.

32. Wyres KL, Cahill SM, Holt KE, Hall RM, Kenyon JJ. 2020. Identification of Acinetobacter baumannii loci for capsular polysaccharide (KL) and lipooligosaccharide outer core (OCL) synthesis in genome assemblies using curated reference databases compatible with Kaptive. Microb Genom 6:e000339. https://doi.org/10.1099/mgen.0.000339.

33. Jolley KA, Bray JE, Maiden MCJ. 2018. Open-access bacterial population genomics: BIGSdb software, the PubMLST.org website and their applications. Wellcome Open Res 3:124. https://doi.org/10.12688/wellcomeopenres.14826.1.

34. Zong Z, Lü X, Valenzuela JK, Partridge SR, Iredell J. 2008. An outbreak of carbapenem-resistant Acinetobacter baumannii producing OXA-23 carbapenemase in western China. Int J Antimicrob Agents 31:50–54. https://doi.org/10.1016/j.ijantimicag.2007.08.019.

35. Figueiredo S, Poirel L, Croize J, Recule C, Nordmann P. 2009. In vivo selection of reduced susceptibility to carbapenems in Acinetobacter baumannii related to ISAba1-mediated overexpression of the natural bla$_{OXA-66}$ oxacillinase gene. Antimicrob Agents Chemother 53:2657–2659. https://doi.org/10.1128/AAC.01663-08.

36. Yamada Y, Suwabe A. 2013. Diverse carbapenem-resistance mechanisms in 16S rRNA methylase-producing Acinetobacter baumannii. J Med Microbiol 62:618–622. https://doi.org/10.1099/jmm.0.048991-0.

37. Coyne S, Courvalin P, Périchon B. 2011. Efflux-mediated antibiotic resistance in Acinetobacter spp. Antimicrob Agents Chemother 55:947–953. https://doi.org/10.1128/AAC.01388-10.

38. Xu C, Bilya SR, Xu W. 2019. adeABC efflux gene in Acinetobacter baumannii. New Microbes New Infect 30:100549. https://doi.org/10.1016/j.nmni.2019.100549.

39. Rosenfeld N, Bouchier C, Courvalin P, Périchon B. 2012. Expression of the resistance-nodulation-cell division pump AdeIJK in Acinetobacter baumannii is regulated by AdeN, a TetR-type regulator. Antimicrob Agents Chemother 56:2504–2510. https://doi.org/10.1128/AAC.06422-11.

40. Jeon JH, Hong MK, Lee JH, Lee JJ, Park KS, Karim AM, Jo JY, Kim JH, Ko KS, Kang LW, Lee SH. 2014. Structure of ADC-68, a novel carbapenem-hydrolyzing class C extended-spectrum β-lactamase isolated from Acinetobacter baumannii. Acta Crystallogr D Biol Crystallogr 70:2924–2936. https://doi.org/10.1107/S1399004714019543.

41. Siguier P, Perochon J, Lestrade L, Mahillon J, Chandler M. 2006. ISfinder: the reference centre for bacterial insertion sequences. Nucleic Acids Res 34:D32–D36. https://doi.org/10.1093/nar/gkj014.

42. Salgado-Camargo AD, Castro-Jaimes S, Gutierrez-Rios R-M, Lozano LF, Altamirano-Pacheco L, Silva-Sanchez J, Pérez-Oseguera Á, Volkow P, Castillo-Ramírez S, Cevallos MA. 2020. Structure and evolution of Acinetobacter baumannii plasmids. Front Microbiol 11:1283. https://doi.org/10.3389/fmicb.2020.01283.

43. Lean SS, Yeo CC. 2017. Small, enigmatic plasmids of the nosocomial pathogen, Acinetobacter baumannii: good, bad, who knows? Front Microbiol 8:1547. https://doi.org/10.3389/fmicb.2017.01547.

44. Ramirez MS, Tolmasky ME. 2010. Aminoglycoside modifying enzymes. Drug Resist Updat 13:151–171. https://doi.org/10.1016/j.drup.2010.08.003.

45. Hamidian M, Hall RM. 2017. Acinetobacter baumannii ATCC 19606 carries GIsul2 in a genomic island located in the chromosome. Antimicrob Agents Chemother 61:e01991-16. https://doi.org/10.1128/AAC.01991-16.

46. Ilyina TS. 2012. Mobile ISCR elements: structure, functions, and role in emergence, increase, and spread of blocks of bacterial multiple antibiotic

resistance genes. Mol Genet Microbiol Virol 27:135–146. https://doi.org/10.3103/S0891416812040040.

47. Nigro SJ, Post V, Hall RM. 2011. The multiresistant Acinetobacter baumannii European clone I type strain RUH875 (A297) carries a genomic antibiotic resistance island AbaR21, plasmid pRAY and a cluster containing ISAba1-sul2-CR2-strB-strA. J Antimicrob Chemother 66:1928–1930. https://doi.org/10.1093/jac/dkr213.

48. Tansirichaiya S, Rahman MA, Roberts AP. 2019. The transposon registry. Mob DNA 10:40. https://doi.org/10.1186/s13100-019-0182-3.

49. Poirel L, Bonnin RA, Boulanger A, Schrenzel J, Kaase M, Nordmann P. 2012. Tn125-related acquisition of blaNDM-like genes in Acinetobacter baumannii. Antimicrob Agents Chemother 56:1087–1089. https://doi.org/10.1128/AAC.05620-11.

50. Bontron S, Nordmann P, Poirel L. 2016. Transposition of Tn125 encoding the NDM-1 carbapenemase in Acinetobacter baumannii. Antimicrob Agents Chemother 60:7245–7251. https://doi.org/10.1128/AAC.01755-16.

51. Zheng X, Zhu J, Zhang J, Cai P. 2020. A novel plasmid-borne tet(X6) variant co-exisiting with blaNDM-1and blaOXA-58 in a chicken Acinetobacter baumannii isolate. J Antimicrob Chemother 75:3397–3399. https://doi.org/10.1093/jac/dkaa342.

52. Balalovski P, Grainge I. 2020. Mobilization of pdif modules in Acinetobacter: a novel mechanism for antibiotic resistance gene shuffling? Mol Microbiol 114:699–709. https://doi.org/10.1111/mmi.14563.

53. Blackwell GA, Hall RM. 2017. The tet39 determinant and the msrE-mphE genes in Acinetobacter plasmids are each part of discrete modules flanked by inversely oriented pdif (XerC-XerD) sites. Antimicrob Agents Chemother 61:e00780-17. https://doi.org/10.1128/AAC.00780-17.

54. Mindlin S, Beletsky A, Mardanov A, Petrova M. 2019. Adaptive dif modules in permafrost strains of Acinetobacter lwoffii and their distribution and abundance among present day Acinetobacter strains. Front Microbiol 10:632. https://doi.org/10.3389/fmicb.2019.00632.

55. D'Andrea MM, Giani T, D'Arezzo S, Capone A, Petrosillo N, Visca P, Luzzaro F, Rossolini GM. 2009. Characterization of pABVA01, a plasmid encoding the OXA-24 carbapenemase from Italian isolates of Acinetobacter baumannii. Antimicrob Agents Chemother 53:3528–3533. https://doi.org/10.1128/AAC.00178-09.

56. Cameranesi MM, Morán-Barrio J, Limansky AS, Repizo GD, Viale AM. 2018. Site-specific recombination at XerC/D sites mediates the formation and resolution of plasmid co-integrates carrying a blaOXA-58- and TnaphA6-resistance module in Acinetobacter baumannii. Front Microbiol 9:66. https://doi.org/10.3389/fmicb.2018.00066.

57. Feng Y, Yang P, Wang X, Zong Z. 2016. Characterization of Acinetobacter johnsonii isolate XBB1 carrying nine plasmids and encoding NDM-1, OXA-58 and PER-1 by genome sequencing. J Antimicrob Chemother 71:71–75. https://doi.org/10.1093/jac/dkv324.

58. Zhou S, Chen X, Meng X, Zhang G, Wang J, Zhou D, Guo X. 2015. "Roar" of blaNDM-1 and "silence" of blaOXA-58 co-exist in Acinetobacter pittii. Sci Rep 5:8976. https://doi.org/10.1038/srep08976.

59. Fu YY, Jiang J, Zhou H, Jiang Y, Fu YY, Yu Y, Zhou J. 2014. Characterization of a novel plasmid type and various genetic contexts of bla OXA-58 in Acinetobacter spp. from multiple cities in China. PLoS One 9:e84680. https://doi.org/10.1371/journal.pone.0084680.

60. Poirel L, Mansour W, Bouallegue O, Nordmann P. 2008. Carbapenem-resistant Acinetobacter baumannii isolates from Tunisia producing the OXA-58-like carbapenem-hydrolyzing oxacillinase OXA-97. Antimicrob Agents Chemother 52:1613–1617. https://doi.org/10.1128/AAC.00978-07.

61. Ang GY, Yu CY, Cheong YM, Yin WF, Chan KG. 2016. Emergence of ST119 Acinetobacter pittii co-harbouring NDM-1 and OXA-58 in Malaysia. Int J Antimicrob Agents 47:168–169. https://doi.org/10.1016/j.ijantimicag.2015.11.008.

62. Bertini A, Poirel L, Mugnier PD, Villa L, Nordmann P, Carattoli A. 2010. Characterization and PCR-based replicon typing of resistance plasmids in Acinetobacter baumannii. Antimicrob Agents Chemother 54:4168–4177. https://doi.org/10.1128/AAC.00542-10.

63. Harmer CJ, Hall RM. 2019. An analysis of the IS6/IS26 family of insertion sequences: is it a single family? Microb Genom 5:e000291. https://doi.org/10.1099/mgen.0.000291.

64. Mollet B, Iida S, Arber W. 1985. Gene organization and target specificity of the prokaryotic mobile genetic element IS 26. Mol Gen Genet 201:198–203. https://doi.org/10.1007/BF00425660.

65. Harmer CJ, Hall RM. 2017. Targeted conservative formation of cointegrates between two DNA molecules containing IS26 occurs via strand exchange at either IS end. Mol Microbiol 106:409–418. https://doi.org/10.1111/mmi.13774.

66. Harmer CJ, Hall RM. 2016. IS26-mediated formation of transposons carrying antibiotic resistance genes. mSphere 1:e00038-16. https://doi.org/10.1128/mSphere.00038-16.

67. Hamidian M, Ambrose SJ, Hall RM. 2016. A large conjugative Acinetobacter baumannii plasmid carrying the sul2 sulphonamide and strAB streptomycin resistance genes. Plasmid 87–88:43–50. https://doi.org/10.1016/j.plasmid.2016.09.001.

68. Hamidian M, Holt KE, Pickard D, Dougan G, Hall RM. 2014. A GC1 Acinetobacter baumannii isolate carrying AbaR3 and the aminoglycoside resistance transposon TnaphA6 in a conjugative plasmid. J Antimicrob Chemother 69:955–958. https://doi.org/10.1093/jac/dkt454.

69. Hamidian M, Hall RM. 2016. The resistance gene complement of D4, a multiply antibiotic-resistant ST25 acinetobacter baumannii isolate, resides in two genomic islands and a plasmid. J Antimicrob Chemother 71:1730–1741. https://doi.org/10.1093/jac/dkw041.

70. Nigro SJ, Hall RM. 2017. A large plasmid, pD46-4, carrying a complex resistance region in an extensively antibiotic-resistant ST25 Acinetobacter baumannii. J Antimicrob Chemother 72:3496–3498. https://doi.org/10.1093/jac/dkx287.

71. Gundi VAKB, Dijkshoorn L, Burignat S, Raoult D, La Scola B. 2009. Validation of partial rpoB gene sequence analysis for the identification of clinically important and emerging Acinetobacter species. Microbiology (Reading) 155:2333–2341. https://doi.org/10.1099/mic.0.026054-0.

72. Clinical and Laboratory Standards Institute. 2020. M100 Performance standards for antimicrobial susceptibility testing, 30th informational supplement, 30th ed. Clinical and Laboratory Standards Institute, Wayne, PA, USA.

73. Bankevich A, Nurk S, Antipov D, Gurevich AA, Dvorkin M, Kulikov AS, Lesin VM, Nikolenko SI, Pham S, Prjibelski AD, Pyshkin AV, Sirotkin AV, Vyahhi N, Tesler G, Alekseyev MA, Pevzner PA. 2012. SPAdes: a new genome assembly algorithm and its applications to single-cell sequencing. J Comput Biol 19:455–477. https://doi.org/10.1089/cmb.2012.0021.

74. Seemann T. 2014. Prokka: rapid prokaryotic genome annotation. Bioinformatics 30:2068–2069. https://doi.org/10.1093/bioinformatics/btu153.

75. Tatusova T, Dicuccio M, Badretdin A, Chetvernin V, Nawrocki EPP, Zaslavsky L, Lomsadze A, Pruitt KDD, Borodovsky M, Ostell J. 2016. NCBI prokaryotic genome annotation pipeline. Nucleic Acids Res 44:6614–6624. https://doi.org/10.1093/nar/gkw569.

76. Diancourt L, Passet V, Nemec A, Dijkshoorn L, Brisse S. 2010. The population structure of Acinetobacter baumannii: expanding multiresistant clones from an ancestral susceptible genetic pool. PLoS One 5:e10034. https://doi.org/10.1371/journal.pone.0010034.

77. Bartual SG, Seifert H, Hippler C, Luzon MAD, Wisplinghoff H, Rodríguez-Valera F. 2005. Development of a multilocus sequence typing scheme for characterization of clinical isolates of Acinetobacter baumannii. J Clin Microbiol 43:4382–4390. https://doi.org/10.1128/JCM.43.9.4382-4390.2005.

78. Page AJ, Cummins CA, Hunt M, Wong VK, Reuter S, Holden MTG, Fookes M, Falush D, Keane JA, Parkhill J. 2015. Roary: rapid large-scale prokaryote pan genome analysis. Bioinformatics 31:3691–3693. https://doi.org/10.1093/bioinformatics/btv421.

79. Price MNN, Dehal PSS, Arkin APP. 2010. FastTree 2—approximately maximum-likelihood trees for large alignments. PLoS One 5:e9490. https://doi.org/10.1371/journal.pone.0009490.

80. Letunic I, Bork P. 2019. Interactive Tree of Life (iTOL) v4: recent updates and new developments. Nucleic Acids Res 47:W256–W259. https://doi.org/10.1093/nar/gkz239.

81. Zankari E, Hasman H, Cosentino S, Vestergaard M, Rasmussen S, Lund O, Aarestrup FM, Larsen MV. 2012. Identification of acquired antimicrobial resistance genes. J Antimicrob Chemother 67:2640–2644. https://doi.org/10.1093/jac/dks261.

82. Alcock BP, Raphenya AR, Lau TTY, Tsang KK, Bouchard M, Edalatmand A, Huynh W, Nguyen AV, Cheng AA, Liu S, Min SY, Miroshnichenko A, Tran HK, Werfalli RE, Nasir JA, Oloni M, Speicher DJ, Florescu A, Singh B, Faltyn M, Hernandez-Koutoucheva A, Sharma AN, Bordeleau E, Pawlowski AC, Zubyk HL, Dooley D, Griffiths E, Maguire F, Winsor GL, Beiko RG, Brinkman FSL, Hsiao WWL, Domselaar GV, McArthur AG. 2020. CARD 2020: antibiotic resistome surveillance with the comprehensive antibiotic resistance database. Nucleic Acids Res 48:D517–D525. https://doi.org/10.1093/nar/gkz935.

83. Xie Y, Wei Y, Shen Y, Li X, Zhou H, Tai C, Deng Z, Ou HY. 2018. TADB 2.0: an updated database of bacterial type II toxin-antitoxin loci. Nucleic Acids Res 46:D749–D753. https://doi.org/10.1093/nar/gkx1033.

84. Bi D, Liu L, Tai C, Deng Z, Rajakumar K, Ou HY. 2013. SecReT4: a web-

based bacterial type IV secretion system resource. Nucleic Acids Res 41:660–665. https://doi.org/10.1093/nar/gks1248.

85. Finn RD, Mistry J, Tate J, Coggill P, Heger A, Pollington JE, Gavin OL, Gunasekaran P, Ceric G, Forslund K, Holm L, Sonnhammer ELL, Eddy SR, Bateman A. 2010. The Pfam protein families database. Nucleic Acids Res 38:D211–D222. https://doi.org/10.1093/nar/gkp985.

86. Marchler-Bauer A, Lu S, Anderson JB, Chitsaz F, Derbyshire MK, DeWeese-Scott C, Fong JH, Geer LY, Geer RC, Gonzales NR, Gwadz M, Hurwitz DI, Jackson JD, Ke Z, Lanczycki CJ, Lu F, Marchler GH, Mullokandov M, Omelchenko MV, Robertson CL, Song JS, Thanki N, Yamashita RA, Zhang D, Zhang N, Zheng C, Bryant SH. 2011. CDD: a Conserved Domain Database for the functional annotation of proteins. Nucleic Acids Res 39:D225–D229. https://doi.org/10.1093/nar/gkq1189.

87. Sullivan MJ, Petty NK, Beatson SA. 2011. Easyfig: a genome comparison visualizer. Bioinformatics 27:1009–1010. https://doi.org/10.1093/bioinformatics/btr039.

88. Grant JR, Stothard P. 2008. The CGView Server: a comparative genomics tool for circular genomes. Nucleic Acids Res 36:W181–184. https://doi.org/10.1093/nar/gkn179.

89. Zhu Y, Lu J, Zhao J, Zhang X, Yu HH, Velkov T, Li J. 2020. Complete genome sequence and genome-scale metabolic modelling of Acinetobacter baumannii type strain ATCC 19606. Int J Med Microbiol 310:151412. https://doi.org/10.1016/j.ijmm.2020.151412.

90. Leungtongkam U, Thummeepak R, Tasanapak K, Sitthisak S. 2018. Acquisition and transfer of antibiotic resistance genes in association with conjugative plasmid or class 1 integrons of Acinetobacter baumannii. PLoS One 13:e0208468. https://doi.org/10.1371/journal.pone.0208468.

91. Christie PJ. 2016. The mosaic type IV secretion systems. EcoSal Plus 7. https://doi.org/10.1128/ecosalplus.ESP-0020-2015.